Seasonal phosphorus and carbon dynamics in a temperate shelf sea (Celtic Sea)

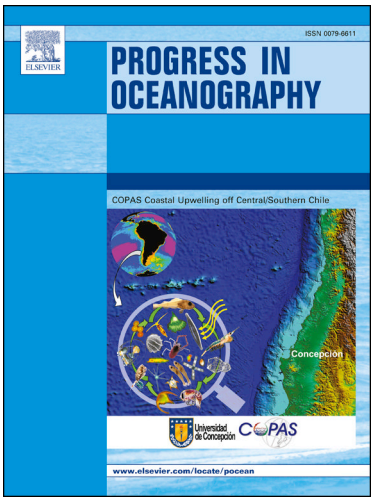

Seasonal phosphorus and carbon dynamics in a temperate shelf sea (Celtic Sea)

Alex J. Poulton, Clare E. Davis, Chris J. Daniels, Kyle M.J. Mayers, Carolyn Harris, Glen A. Tarran, Claire E. Widdicombe, E. Malcolm S. Woodward

PII: S0079-6611(17)30158-1
DOI: https://doi.org/10.1016/j.pocean.2017.11.001
Reference: PROOCE 1872

To appear in: *Progress in Oceanography*

Please cite this article as: Poulton, A.J., Davis, C.E., Daniels, C.J., Mayers, K.M.J., Harris, C., Tarran, G.A., Widdicombe, C.E., Woodward, E.M.S., Seasonal phosphorus and carbon dynamics in a temperate shelf sea (Celtic Sea), *Progress in Oceanography* (2017), doi: https://doi.org/10.1016/j.pocean.2017.11.001

Seasonal phosphorus and carbon dynamics in a temperate shelf sea (Celtic Sea)

Alex J. Poulton[1,†], Clare E. Davis[2], Chris J. Daniels[1], Kyle M.J. Mayers[3], Carolyn Harris[4], Glen A. Tarran[4], Claire E. Widdicombe[4], and E. Malcolm S. Woodward[4]

[1] National Oceanography Centre, Waterfront Campus, Southampton, UK

[2] Department of Earth, Ocean and Ecological Sciences, University of Liverpool, Liverpool, UK

[3] Ocean and Earth Science, University of Southampton, National Oceanography Centre Southampton, Southampton, UK

[4] Plymouth Marine Laboratory, Prospect Place, The Hoe, Plymouth, UK

[†] Current address: The Lyell Centre, Heriot-Watt University, Edinburgh, UK

* Corresponding author.

Tel: +44 (0) 131 451 3891.

Email address: a.poulton@hw.ac.uk

Highlights:

- Seasonal uptake of phosphorus (P) and its dissolved organic release examined in Celtic Sea
- Uptake highest in spring bloom, with biomass-normalised affinity highest in summer
- Release high in November and late spring, with efficient P-retention and recycling in summer
- Strong phytoplankton influence on spring P-uptake, whilst bacteria influential in summer
- Relatively C-rich uptake in November and late April, P-rich in summer and early April

Abstract

The seasonal cycle of resource availability in shelf seas has a strong selective pressure on phytoplankton diversity and the biogeochemical cycling of key elements, such as carbon (C) and phosphorus (P). Shifts in carbon consumption relative to P availability, via changes in cellular stoichiometry for example, can lead to an apparent 'excess' of carbon production. We made measurements of inorganic P (P_i) uptake, in parallel to C-fixation, by plankton communities in the Celtic Sea (NW European Shelf) in spring (April 2015), summer (July 2015) and autumn (November 2014). Short-term (<8 h) P_i-uptake coupled with dissolved organic phosphorus (DOP) release, in parallel to net (24 h) primary production (NPP), were all measured across an irradiance gradient designed to typify vertically and seasonally varying light conditions. Rates of P_i-uptake were highest during spring and lowest in the low light conditions of autumn, although biomass-normalised P_i-uptake was highest in the summer. The release of DOP was highest in November and declined to low levels in July, indicative of efficient utilization and recycling of the low levels of P_i available. Examination of daily turnover times of the different particulate pools, including estimates of phytoplankton and bacterial carbon, indicated a differing seasonal influence of autotrophs and heterotrophs in P-dynamics, with summer conditions associated with a strong bacterial influence and the early spring period with fast growing phytoplankton. These seasonal changes in autotrophic and heterotrophic influence, coupled with changes in resource availability (P_i, light) resulted in seasonal changes in the stoichiometry of NPP to daily P_i-uptake (C:P ratio); from relatively C-rich uptake in November and late April, to P-rich uptake in early April and July. Overall, these results highlight the seasonally varying influence of both autotrophic and heterotrophic components of shelf sea ecosystems on the relative uptake of C and P.

Keywords: Phosphorus; Phosphate uptake; Dissolved organic Phosphorus; Stoichiometry.

Regional index terms: Celtic Sea; Northwest European Shelf.

1. Introduction

Phosphorus (P) is an essential nutrient for marine organisms, forming an important component of various cellular constituents, including cell membranes and nucleic acids (RNA, DNA), and in the transmission of chemical energy (Benitez-Nelson, 2000; Karl, 2000; Dyhram et al., 2007). The availability of P has an important role in controlling planktonic biomass and production and community composition (Karl et al., 2001), with regionally low (pM) P concentrations limiting biomass accumulation and biogeochemical processes (Moore et al., 2013). The biological cycling of nutrients (P, N) are strongly coupled to the carbon (C) cycle via plankton biomass, resulting in biological processes, such as photosynthesis and respiration, having a strong influence on atmospheric CO_2 (Sterner and Elser, 2002; Arrigo, 2005).

The elemental stoichiometry (C:P, C:N) of plankton propagates through marine food webs to shape ecosystem structure and function (Sterner and Elser, 2002; Elser et al., 2003), and hence plankton provide an interface linking biogeochemical cycles, ecosystem dynamics and global climate (Arrigo, 2005; Finkel et al., 2010). Understanding microbial elemental stoichiometry is important as these relationships play major roles in coupled elemental cycles (Falkowski and Davis, 2004). Planktonic micro-organisms, such as heterotrophic bacteria and phytoplankton, have rapid growth rates and hence can exert a strong influence on the turnover of different C, N and P pools (Arrigo, 2005). Both phytoplankton and heterotrophic bacteria consume P, though the two have different roles in the marine C-cycle as primary producers and remineralisers of organic material respectively (Duhamel and Moutin, 2009), and they may compete strongly for available P when it is in short supply (Thingstad et al., 1993, 1996).

In the marine environment, P is mainly found in dissolved inorganic and organic forms as well as in particulate organic matter such as algal cells and detrital material. P is found in the form of phosphate (P_i) with P predominately entering the ocean through rivers, and with the main losses being through sedimentary processes (Benitez-Nelson, 2000; Karl, 2000; Dyhram et al., 2002). The production of DOP is via cellular exudation or lysis, as part of the production of dissolved organic matter. Microbes directly incorporate P_i, though a small proportion of dissolved organic phosphorus (DOP) may also be bioavailable and must be hydrolysed to be incorporated into the cell (Benitez-Nelson, 2000).

In coastal waters, DOP concentrations range from 0 to 50% of the total P pool, while in the open ocean it can be as high as 75% (Karl and Tien, 1992; Benitez-Nelson, 2000; Bjorkman et al., 2000; Lønborg et al., 2009; Davis et al., 2014). Not all DOP is labile or bioavailable, with its availability for biological uptake controlled by its chemical composition, and up to 50% of the DOP can be

refractory and inactive (Bjorkman et al., 2000; Bjorkman and Karl, 2003; Dyhram et al., 2007; Lønborg et al., 2009). The turnover rates of P within dissolved and particulate pools may be rapid (from a few days to a couple of weeks), and vary over seasonal timescales, allowing low P to support relatively high rates of primary production in coastal waters (Benitez-Nelson and Buesseler, 1999).

Redfield (e.g., Redfield et al., 1963) proposed that plankton and particulate material have a relatively constrained elemental ratio (C:N:P) of 106:16:1, which matches closely with the average ratio of dissolved inorganic N and P in seawater. These observations led to the paradigm that plankton consume inorganic N and P in the same proportion as their availability, fixing them into particulate organic material that is eventually decomposed, thus returning N and P back into their inorganic forms (e.g., Redfield et al., 1963). This paradigm of elemental stoichiometry has been used to link plankton production to the biogeochemical cycling of C, N and P. However, important deviations from the canonical Redfield ratio may occur in the biochemical composition of marine plankton (e.g., Geider and La Roche, 2002; Ho et al., 2003; Finkel et al., 2010), trophic interactions (e.g., Sterner and Elser, 2002; Hessen et al., 2002, 2004) and biogeochemical processes (e.g., Arrigo, 2005; Bozec et al., 2006; Bauer et al., 2013).

As different cellular components, such as proteins and pigments, have their own stoichiometric characteristics and represent significant amounts of the material in plankton cells, changes in their relative proportions strongly influence bulk stoichiometry (Falkowski, 2000; Geider and La Roche, 2002). Under nutrient limited growth conditions plankton show increased cellular quotas of C, suggesting increased uptake and storage of C-rich compounds (e.g., Geider and La Roche, 2002). Rapid growth rates are predicted to lead to P-rich biomass as the cellular components required for cell division have a high P-content (i.e., ‘the growth rate hypothesis’; Sterner and Elser, 2002). Variability in phytoplankton cellular composition (chlorophyll content, elemental stoichiometry) also influences their quality as food items for higher trophic levels, and affects their growth rates and trophic transfer efficiency (e.g., Hessen et al., 2002, 2004; Sterner and Elser, 2002).

The role of variable elemental stoichiometry is an important factor in determining the C-sequestration efficiency of the Continental Shelf Pump (CSP) (Thomas et al., 2004, 2005; Bozec et al., 2006). The CSP describes the process whereby CO_2, as dissolved inorganic carbon (DIC), is transformed into particulate organic carbon (via photosynthesis) in the upper water column, exported below the thermocline where it is remineralised back into DIC, and then this DIC is advected into the adjacent open-ocean during winter time convective mixing (Thomas et al., 2004, 2005; Bozec et al., 2006). The efficiency of the CSP may be regulated by changing the ratio of nutrient utilization for photosynthesis and production of particulate material, and by changing the

ratio of nutrient recycling and DIC remineralisation. For example, seasonal changes in DIC and nutrient drawdown in the North Sea have shown that C-overconsumption occurs relative to nutrient utilization, assuming Redfield stoichiometry (Toggweiler et al., 1993; Thomas et al., 2004, 2005; Bozec et al., 2006; Kühn et al., 2010). Such C-overconsumption has been suggested to relate to changes in plankton stoichiometry under seasonally varying resource availability (Toggweiler et al., 1993; Thomas et al., 2004, 2005; Bozec et al., 2006; Kühn et al., 2010). Under nutrient limited conditions plankton may show elevated, relative to the Redfield ratio, C-rich uptake and cellular quotas, and release C-rich dissolved organic matter (e.g., Geider and La Roche, 2002; López-Sandoval et al., 2011). However, direct measurements have yet to confirm whether C-overconsumption in the CSP is a direct consequence of plankton stoichiometry or whether other biogeochemical processes (e.g. nutrient recycling) are more influential on CSP efficiency. The stoichiometry of primary production, nutrient uptake and recycling, trophic transfer and decomposition, are all likely to influence the metabolic balance of shelf seas and the efficiency of the CSP to varying degrees (Bauer et al., 2013).

Shelf seas represent less than 10% of the global ocean area, but are responsible for 10 to 30% of primary production, as well as high proportions of global carbon sequestration (Joint et al., 2001; Simpson and Sharples, 2012; Bauer et al., 2013). Hence, determining the processes that underpin the magnitude and efficiency of the CSP is an important step in understanding how shelf seas attain and maintain these roles with environmental variability. The aims of the present study were to: (1) explore seasonal patterns in P_i-uptake and P-release (DOP production) relative to variability in water-column structure, nutrient (N, P) availability, and plankton community composition; and (2) examine the dynamics of P-biogeochemistry in terms of the turnover of different P pools and the stoichiometry of P_i-uptake relative to C-fixation (net primary production, NPP). Overall, this paper provides a better understanding of how the internal biogeochemical cycling of elements contribute to the maintenance and efficiency of the CSP in the Celtic Sea. The specific hypotheses examined are that: (a) the optimal growth conditions of the spring bloom lead to C-fixation and P_i-uptake at ratios close to the Redfield ratio; whilst (b), departures from the Redfield ratio occur in response to changes in resource (light, nutrient) availability.

2. Methods

2.1. Sampling

This study presents data collected from three cruises on-board the *RRS Discovery* to the Celtic Sea over the period 2014 to 2015; the first in November 2014 (DY018: 9th November to 2nd December), the second in spring 2015 (DY029: 1st April to 29th April), and the third and final

cruise in summer 2015 (DY033: 11th July to 2nd August). Each cruise focused on a different time-period relevant to the ecosystem and biogeochemistry of the Celtic Sea, from the spring-bloom (April) to summer stratified period (July), and onto the late autumn bloom and break down of stratification (November). As part of this study, two sites were sampled for phosphate dynamics and ancillary parameters, with the main site in the Central Celtic Sea (CCS; ~49^{o}24' N, 8^{o}36'W; 150 m water depth), and the second at the Shelf Break (CS2; ~48^{o}34.26'W, 9^{o}30.58' W; 203 m water depth) (Fig. 1). Over the three sampling periods these sites were repeatedly sampled, though CCS was more frequently sampled (n = 15) than CS2 (n = 6).

Water samples were collected from six light depths in 20 L Niskin bottles on a CTD rosette sampler deployed pre-dawn (02:00-06:00 h local time) at CCS and CS2. The light depths sampled were 60, 40, 20, 10, 5 and 1% of surface irradiance (Photosynthetically Active Radiation, PAR). Pre-dawn sampling depths were determined by back calculation of the vertical attenuation coefficient of PAR (K_d, m^{-1}), based on either: (a) an assumption that the base of the surface mixed layer (thermocline) was at or close to the depth of the euphotic zone (i.e. 1% of surface irradiance) (November, April); or (b) that the sub-surface chlorophyll-*a* maximum (SCM) occurred at or close to a depth of 5% of surface irradiance (July) (Hickman et al., 2012).

Surface mixed layer (SML) depths were determined from processed CTD density data (J. Hopkins, Liverpool, pers. comm.) through a two-step process. Firstly, SMLs were identified automatically by applying a threshold for change in potential density with depth (an increase of either 0.02 kg m^{-3} (November, July) or 0.01 kg m^{-3} (April) from the potential density at 10 m (or the nearest available measurement)). Secondly, visual examination and confirmation for profiles that failed these criteria or were close to the thresholds selected. Automatic detection of SML depths was successful at CCS, though there were issues at CS2 due to internal wave breaking, and at CCS during April as the stratification of the water-column evolved (J. Hopkins, Liverpool, pers. comm.). Identification of the thermocline during the cruise was based on unprocessed CTD temperature data, while SML identification was based on processed CTD density data. Hence, differences in SML and euphotic zone depths during November and April are possible due to discrepancies in these data sources and physical complexities of the water-column (especially during April and at the shelf break).

2.2. Incubations

Water samples for NPP, P_i-uptake and DOP production were all incubated in a purposely converted and refitted commercial 20 foot ISO refrigeration shipping container (see Richier et al., 2014), allowing incubation temperatures to be regulated at in situ values (± 1-2^{o}C). Each of the six percentage light depths (60, 40, 20, 10, 5 and 1% of surface irradiance) had a dedicated incubation

chamber built, using blackout material to remove any light contamination between the different light chambers. Irradiance was provided by one to three daylight simulation LED panels (Powerpax, UK), each providing up to 100 µmol quanta m^{-2} s^{-1}, combined with different types of neutral density filters (Lee Filters^{TM}, UK). The light-dark cycle was varied between different cruises to accurately represent seasonal variability in photoperiods; 9 h in November, 14 h in April and 16 h in July.

To determine the seasonal range in incidental irradiance and allow representative daily light doses to be determined for each light depth and each cruise, weekly average daily PAR levels (mol quanta m^2 d^{-1}) over a ten-year period (2003 to 2013) was determined from MODIS Aqua data (S. Henson, Southampton, pers. comm.). Monthly averages over the ten years for incidental irradiance (E_0) for each cruise period were then calculated for the position of the CCS site, giving values of 9.4 mol quanta m^{-2} d^{-1} (November), 36.8 mol quanta m^{-2} d^{-1} (April), and 43.2 mol quanta m^{-2} d^{-1} (July). Actual irradiance levels (E_0) during each cruise were measured by an on board *RRS Discovery 2π* PAR irradiance sensor (Skye Instruments, SKE 510), with cruise averages (Table 1) showing excellent agreement with long-term monthly averages.

Incidental irradiances for each month were corrected for reflective losses at the sea surface, assuming an 8% loss (D. McKee, Strathclyde, pers. comm.) to give incidental irradiance (100%) values and allow calculation of a light dose for each percentage irradiance chamber. Daily light doses (mol quanta m^{-2} d^{-1}) were reconstructed using a combination of LED panels and neutral density filters, to achieve a target incidental irradiance per incubation chamber of 7 to 440 µmol quanta m^{-2} s^{-1}, which were combined with the appropriate seasonal photoperiod to give a representative seasonal daily light dose for each percentage light depth (see Supplementary Table S1).

In summer, when strong vertical stratification occurred across the euphotic zone, the deeper light depth (1%) samples were incubated in a Fytoscope FS130 laboratory incubator (Photon System Instr., Czech Republic) at in situ temperatures (± 1^{o}C) and with a white LED light panel to replicate the required light dose (see Supplementary Table S1). All light levels in the incubation chambers and Fytoscope were checked with a *4π* scalar PAR irradiance sensor (Biophysical Instruments, QSL-2101).

Incubations for inorganic phosphate uptake and dissolved organic phosphorus release were short-term (<8 h; see below) and hence it is not appropriate to consider patterns in these rates against the full daily light-dose experienced over the entire day-length. Rather, in this study, uptake and release rates are presented (Figs. 2, 3, 4 and 6) against gradients in instantaneous irradiance (h^{-1}), but not

daily photon flux periods (d^{-1}). One important consequence of this is that seasonal changes in day-length have no influence on the vertical patterns in uptake or release rates.

2.3. Inorganic Phosphate Uptake and Release of Dissolved Organic Phosphorus

Hourly rates (dawn to midday, ~6-8 h) of inorganic phosphate uptake (P_i-uptake) were determined following Rees et al. (1999), Björkman et al. (2000), and Reynolds et al. (2014). Water samples from the six light depths were collected directly from the CTD under low-light conditions (pre-dawn) into 500 mL brown Nalgene™ bottles which were returned to the on-board laboratory for sub-sampling. Under low light conditions, sub-samples (3 light, 1 dark) were then dispensed into 70 mL polycarbonate bottles (Corning, Inc.) and each bottle spiked with either 111 to 222 kBq ^{33}P-labelled orthophosphoric acid (PerkinElmer, Inc., specific activity 37 kBq $nmol^{-1}$) during April 2015 and November 2014, or 333 kBq ^{33}P-labelled orthophosphoric acid (Hartman Analytical GmbH, specific activity 111 kBq $pmol^{-1}$) during July 2015. Use of these two isotopes ensured low P_i addition and no enrichment of the ambient P_i pools; in the case of April and November the spike addition resulted in ~3 to 6 nmol P (<3% of ambient P_i concentrations), and ~9 pmol in July (<1% of ambient P_i concentrations). From one light bottle per light depth, three aliquots of 100 µL were then removed and placed into 7 mL glass scintillation vials to which 6 mL of Ultima Gold™ (PerkinElmer, Inc.) liquid scintillation cocktail was added, and initial activities were counted at sea on a Tri-Carb 3110TR scintillation counter. Triplicate light bottles and the single dark bottle were then incubated in the controlled temperature (CT) incubators for 6 to 8 h at six irradiance levels (see previous Section).

To determine P_i-uptake, incubations were terminated by filtration of each sample bottle (3 light, 1 dark) onto a 25 mm diameter 0.45 µm polycarbonate Nuclepore™ filter under gentle pressure. Filtered samples were rinsed with unlabelled Whatman GF/F filtered seawater, air-dried and placed in 7 mL glass scintillation vials and 6 mL of Ultima Gold™ (PerkinElmer, Inc.) liquid scintillation cocktail added. Activity on the filters was then determined on a Tri-Carb 3100TR scintillation counter, with P_i-uptake calculated following Björkman et al. (2000). P_i-uptake is represented both on hourly time-scales (Fig. 3), averaged from the short-term (6-8 h) incubations, and scaled to a daily (24 h) time-frame (Table 2) by multiplying hourly rates by 24 and assuming little or no diurnal variability in P_i-uptake (see Discussion).

To determine the release of Dissolved Organic Phosphorus (DOP), at the end the incubation period 10 mL aliquots were removed from each of the four sample bottles (3 light, 1 dark) from three light depths (60, 20 and 1% during November and April, 60, 5 and 1% during July). These aliquots were gently filtered through 25 mm diameter 0.2 µm Whatman Nuclepore™ polycarbonate filters to

remove particulate material and the filtrate caught in 15 mL glass test tubes (10% Hydrochloric acid-washed, Milli-Q-rinsed and oven-dried). Each 10 mL aliquot was then transferred to a plastic 15 mL centrifuge tube and 250 µL of a 1 M sodium hydroxide solution (Sigma-Aldrich, UK) added to precipitate out the dissolved P_i and leave the ^{33}P-labelled DOP (Karl and Tien, 1992; Thomson-Bulldis and Karl, 1998; Björkman et al., 2000). Aliquots were shaken vigorously and centrifuged for 1 h at 3500 rpm, with 1 mL of the supernatant removed from each, and placed in 7 mL glass scintillation vials with 6 mL of Ultima Gold^{TM} (PerkinElmer, Inc.) liquid scintillation cocktail. The activity of the filtrate was then measured in a TriCarb 3100TR scintillation counter.

To estimate the proportion of DOP exuded relative to the phosphate (P_i) consumed, the gross rate of P_i-uptake was estimated as the rate of P_i-uptake plus the rate of DOP production. Hence, we calculated a percentage extracellular release for DOP as the fraction of total P_i-uptake (i.e., the sum of P_i-uptake and DOP production) represented by DOP production alone, multiplied by 100. DOP production is represented both on hourly time-scales (Fig. 4), averaged from the short-term (6-8 h) incubations, and scaled to a daily (24 h) time-frame by multiplying hourly rates by 24 and assuming little or no diurnal variability in DOP production.

The average relative standard deviation (RSD = standard deviation/Average x 100) of triplicate P_i-uptake measurements was 13% (range 2-49%) for November, 18% (3-67%) for April and 18% (1-66%) for July. The average RSD of triplicate DOP production measurements was 31% (1-94%) for November, 17% (1-39%) for April and 20% (2-53%) for July.

2.5. Particulate Organic Phosphorus and Dissolved Organic Phosphorus

Water samples for determination of the concentrations of Particulate Organic Phosphorus (POP) were collected from 6 to 8 depths (see Davis et al., this issue). Water samples (1 L) for POP concentrations were filtered onto 25 mm Whatman GF/F (pre-combusted for 4 h at 450^{o}C and Hydrochloric acid-washed) glass-fibre filters (nominal pore size 0.7 µm) on a plastic filtering rig under less than 12 kPa vacuum pressure. Filters were dried and POP concentrations determined following Davis et al. (2014, this issue), with analysis in duplicate against certified reference materials (CRM; SRM 1515 Apples Leaves, NIST) in triplicate with each sample extraction to ensure analytical precision and accuracy of less than 2%. Sampling and storage bottles for POP and DOP were pre-cleaned with 10% Hydrochloric acid and rinsed with Milli-Q before use. Samples for DOP were pre-filtered through a combusted and acid-rinsed Whatman GF/F filter and stored in HDPE bottles at -20^{o}C before analysis. DOP concentrations were determined in triplicate by measuring the difference in phosphate concentration before (total phosphate) and after (total dissolved phosphate) UV oxidation.

Total dissolved phosphorus (TDP) was determined using the high temperature acid persulfate technique as described in Lomas et al. (2010) with the following modifications. Standards were made up in P-free artificial seawater using potassium monobasic phosphate ($KHPO_4$, Sigma Aldrich). Samples and standards were autoclaved (121°C, 40 min) as 40 mL aliquots in tightly sealed 50 mL glass Pyrex® bottles with Teflon® lined screw caps after addition of 5 mL potassium persulfate solution (64 g/L). Following oxidation, samples were cooled overnight and then precipitated using the magnesium induced co-precipitation (MAGIC) method (Karl and Tien, 1992) by addition of 5 mL 1M sodium hydroxide solution (Sigma Aldrich). This step removed chloride ions, which appeared to cause interference during DIP determination. Following centrifugation (1000 x g, 60 min), the supernatant was discarded and the sample/standard pellet was completely dissolved in 40 mL 0.1 M hydrochloric acid (Trace metal grade, Sigma Aldrich). Analytical blanks were determined as described in Lomas et al. (2010).

Total dissolved phosphorus was determined in triplicate as dissolved inorganic phosphorus (DIP) concentrations in the samples by the molybdenum blue method (Murphy and Riley, 1962) using a Bran and Luebbe QuAAtro 5-channel auto-analyser (DIP detection limit 50 nM). At low DIP concentrations (<100 nM), samples were reanalysed in triplicate 50 mL aliquots using the MAGIC method (Karl and Tien, 1992) prior to DIP determination as above (detection limit 20 nM DIP). Dissolved organic phosphorus (DOP) was quantified as the difference in DIP concentrations before and after persulfate oxidation (i.e. DOP = TDP - DIP; DOP detection limit 40 nM).

2.6. Nutrients and Chlorophyll-a

Water samples for determination of nutrient concentrations (nitrate+nitrite, nitrite, phosphate, and silicic acid) were collected directly from the CTD into aged, acid-washed and Milli-Q-rinsed 60 mL HDPE Nalgene™ bottles. Clean sampling and handling techniques were employed during the sampling and manipulations within the laboratory, and where possible carried out according to the International GO-SHIP nutrient manual recommendations (Hydes et al., 2010). Nutrient samples were all analysed on board the *RRS Discovery* using a Bran and Luebbe segmented flow colorimetric auto-analyser using techniques described in Woodward and Rees (2001). Nutrient reference materials (KANSO Japan) were run each day to check analyser performance and to guarantee the quality control of the final reported data. The typical uncertainty of the analytical results were between 2 to 3%, and the limits of detection for nitrate and phosphate was 0.02 µmol L^{-1}, nitrite 0.01 µmol L^{-1}, whilst silicic acid was always higher than the limits of detection. Further details of the nutrient analysis and seasonal variability in nutrient inventories can be found in Humphreys et al. (this issue).

Water samples (0.2-0.25 L) for chlorophyll-*a* extraction were filtered onto 25 mm diameter Whatman GF/F or Fisherbrand MF300 glass fibre filters (effective pore sizes 0.7 µm) and extracted in 6 to 10 mL 90% acetone (HPLC grade, Sigma-Aldrich, UK) at -4^{o}C for 18 to 24 h (Poulton et al., 2014). Fluorescence was measured on a Turner Designs Trilogy fluorometer using a non-acidification module and calibrated with a solid standard and a pure chlorophyll-*a* standard (Sigma-Aldrich, UK).

2.7. Primary Production

Daily rates (dawn to dawn, 24 h) of primary production (i.e. Net Primary Production (NPP)) included in this paper were determined following the methodology outlined by Mayers et al. (this issue) and Poulton et al. (2014). Seawater samples were collected from the same six light depths as for P_i-uptake (see Section 2.3), directly from 20 L Niskin bottles on the CTD rosette into 500 mL brown Nalgene^{TM} bottles (10% Hydrochloric acid-washed, Milli-Q-rinsed) and transferred under low light conditions to the on-board laboratory. In the laboratory, four (3 light, 1 formalin-killed blank) 70 mL polycarbonate (Corning^{TM}) bottles were filled per light depth. Carbon-14 (^{14}C) labelled sodium bicarbonate (1258-1628 kBq) was added to each bottle and then three of the bottles were incubated at the relevant light level in the CT container for 24 h (see Section 2.2). The fourth sample (formalin-blank) had 1 mL of borate buffered formaldehyde (~1% final concentration) added and was incubated alongside the other samples to measure abiotic uptake.

Incubations were terminated by filtering onto 25 mm 0.45 µm Whatman Nuclepore^{TM} polycarbonate filters, with extensive rinsing to remove any unfixed ^{14}C-labelled sodium bicarbonate remaining on the filters. Organic (NPP) carbon fixation was determined using the micro-diffusion technique (see Mayers et al., this issue) in 20 mL glass vials with 1 mL of 1% orthophosphoric acid added to remove any ^{14}C-particulate inorganic carbon, and 10 to 15 mL of Ultima Gold^{TM} (PerkinElmer, Inc.) liquid scintillation cocktail added to each sample. The activity on the filters was then determined on a Tri-Carb 3100TR liquid scintillation counter on-board. Spike activity was checked by removal of triplicate 100 µL subsamples directly after spike addition and mixing with 200 µL of β-phenylethylamine (Sigma-Aldrich, UK) followed by Ultima Gold^{TM} addition and liquid scintillation counting. The average RSD of triplicate NPP measurements was 15% (2-44%) for November, 14% (1-59%) for April and 11% (1-42%) for July. The formalin blank consistently represented less than 2% of NPP rates (cruise averages: 2%, November; 2%, April; 1%, July).

2.8. Phytoplankton and Bacterial Carbon

Cell abundances for the major phytoplankton groups were analysed from each sampling depth within the euphotic zone, through either flow cytometry (for *Synechococcus*, pico-eukaryotes, nano-

eukaryotes, coccolithophores, cryptophytes, and bacteria) or light microscopy (for diatoms and autotrophic dinoflagellates). Samples for flow cytometry were collected in clean 250 mL polycarbonate bottles and analysed using a Becton Dickinson FACSort instrument (Tarran et al., 2006) while samples for light microscopy were collected in 250 mL brown glass bottles and preserved in acidic Lugol's solution (2% final solution) until analysis under an Olympus DMI4000B microscope (Widdicombe et al., 2010).

Cell abundances from flow cytometer counts were converted to biomass using literature values (Tarran et al., 2006): specifically, 8.58 fmol C cell^{-1} for *Synechococcus*, 2.7 fmol C cell^{-1} for *Prochlorococcus*, 36.67 fmol C cell^{-1} for pico-eukaryotes, 0.76 pmol C cell^{-1} for nano-eukaryotes, 1.08 pmol C cell^{-1} for coccolithophores, and 1.97 pmol C cell^{-1} for cryptophytes. Heterotrophic bacteria counts were converted to biomass using values of 1.58 fmol C cell^{-1} for 'High Nucleic Acid'-containing cells and 0.91 fmol C cell^{-1} for 'Low Nucleic Acid'-containing cells. Cellular biomass for light microscope counted taxa (diatoms and autotrophic dinoflagellates), were estimated from cell dimensions following Kovala and Larrence (1966) on an individual species basis. For the estimates of phytoplankton carbon used in this study, a geometric mean value for all the species present in the Celtic Sea samples was used: specifically, 19.58 pmol C cell^{-1} for diatoms and 85.25 pmol C cell^{-1} for autotrophic dinoflagellates.

3. Results

3.1. Seasonal changes in environmental conditions in the Celtic Sea

Clear seasonal variability (Table 1) at both study sites (CCS, CS2) was evident in terms of changes in the depth and average temperature of the surface mixed layer (SML), as well as the surface concentration of inorganic phosphate (P_i) and nitrate+nitrite (NO_x). The SML shallowed from ~50 m to ~20 to 30 m and warmed by ~6^{o}C between April and July, while it was at its deepest (average 50 m) and at intermediate temperatures (12.8-13.9^{o}C) in November (Table 1). Nutrient concentrations (both P_i and NOx) were highest in early April and declined into low nutrient (P_i <100 nmol P L^{-1}; NO_x <20 nmol N L^{-1}) summer conditions in July (Table 1). Significant temporal variability was also observed throughout April, with the SML shallowing (from 51 to 16 m) and warming by ~1^{o}C, accompanied by the drawdown of both P_i (~300 nmol P L^{-1}) and NO_x (5.5 µmol N L^{-1}). The ratio of NO_x to P_i, expressed as the deficit of NO_x relative to that expected if the two where in Redfield proportions (i.e. $N^* = NO_x – (16 \times P_i)$; see Moore et al., 2009), showed that shelf waters were almost always depleted (relative to the Redfield ratio) in terms of NO_x, with most N* values well below zero across all three sampling periods (Table 1). In fact, the N* values per cruise were very similar, with little seasonal variability, whereas the absolute N:P ratio (mol:mol) was low

379 in November and April (~8-12 and 3-12, respectively) and extremely low (<0.5) in July (data not
380 shown; see also Humphreys et al., this issue).

381 Seasonal patterns were also obvious in terms of incidental irradiance (E_0) and SML average
382 irradiance ($\bar{E}_{SML}$), with both increasing from November to April and July (Table 1). November had
383 noticeably lower irradiance levels relative to both April and July, with the latter two months having
384 very similar irradiance levels despite differences in day length and euphotic zone depths (Table 1).
385 Euphotic zone depths in November were similar to SML depths, whereas SML depths were
386 generally shallow than euphotic zone depths in late April and July. Increasing $\bar{E}_{SML}$ in April, in
387 parallel with nutrient drawdown, was associated with a shallowing of the SML rather than
388 increasing E_0, and highlights the role of water-column structure in spring bloom development
389 (Table 1).

390 Discrete measurements of P_i over the euphotic zone also showed clear seasonal variability between
391 the sampling periods (Fig. 2a), with vertical differences absent in November and April but clearly
392 present in July. Concentrations of P_i were highest in April (up to 500 nmol P L^{-1}), varying from
393 ~200 to 500 nmol P L^{-1} over the month, and lowest (<100 nmol P L^{-1}) in July, apart from at the base
394 of the euphotic zone (>100-600 nmol P L^{-1}) associated with a nutricline (Fig. 2a) and a Sub-surface
395 Chl-*a* Maximum (SCM; Fig. 2b). Euphotic zone Chl-*a* concentrations were also uniform with
396 sampling depth in November and April, while a SCM was evident in July with deep Chl-*a*
397 concentrations ranging from ~0.5 to 2.25 mg m^{-3} (Fig. 2b). The highest Chl-*a* concentrations, and
398 greatest variability, were observed in April during the spring bloom, with Chl-*a* at depth ranging
399 from ~1 to 8 mg m^{-3} (Fig. 2b). A slight variation to this pattern in April was observed at the deepest
400 sampling depth where Chl-*a* concentrations were consistently low (1-2 mg m^{-3}) and similar to
401 concentrations at depth in November (Fig. 2b).

402 In terms of DOP concentrations (Fig. 2c), average discrete depth measurements in the euphotic zone
403 were high and relatively similar in November (266 to 389 nmol P L^{-1}) and April (241 to 438 nmol P
404 L^{-1}), but slightly lower in July (169 to 271 nmol P L^{-1}). No distinct depth pattern was evident
405 between November, April or July, with upper euphotic zone measurements similar to those found at
406 the base of the euphotic zone. In contrast to DOP, POP concentrations showed a different temporal
407 pattern, with the highest (> 75 nmol P L^{-1}) concentrations in April rather than November or July
408 (<75 nmol P L^{-1}), though this trend was most clearly seen in the upper sampling depths of the
409 euphotic zone (Fig. 2d). Average POP concentrations in April in the upper euphotic zone ranged
410 from 91 to 133 nmol P L^{-1}, with averages in November and July ranging from 28 to 46 nmol P L^{-1}
411 and 23 to 51 nmol P L^{-1}, respectively.

3.2. Vertical profiles of Phosphate uptake

Discrete measurements of P_i-uptake over the euphotic zone (Fig. 3a) also showed clear seasonal differences, with rates in April (>1.5 nmol P L^{-1} d^{-1}) much higher than those in July (<1.5 nmol P L^{-1} d^{-1}) or November (<0.4 nmol P L^{-1} d^{-1}). Upper euphotic zone P_i-uptake rates ranged from 1.2 to 5.1 nmol P L^{-1} h^{-1} in April, 0.5 to 2.1 nmol P L^{-1} h^{-1} in July and 0.2 to 0.4 nmol P L^{-1} h^{-1} in November. Uptake of P_i across the incubation light gradients showed light-dependent variability in both November and April, being highest at the higher irradiance levels and decreasing with declining irradiance (Fig. 3a). In contrast, P_i-uptake in July showed no dependency on incubation irradiance despite the absolute irradiance levels being identical to April, most likely due to limiting P_i concentrations in July (Fig. 2a) and hence substrate rather than irradiance dependency.

The ratio of light P_i-uptake to dark P_i-uptake was most often greater than 1, especially at irradiance levels greater than ~0.4 mol quanta m^{-2} h^{-1} during all three sampling periods (Fig. 3b). Ratios of light to dark P_i-uptake were only less than 1 at the very lowest irradiance levels (<0.1 mol quanta m^{-2} h^{-1}) in November and April, whereas ratios rarely fell below 1 (or 1.5) during July. Ratios near unity for light to dark P_i-uptake highlight how there was very little difference between light and dark P_i-uptake rates in November and April, whereas a difference was more noticeable in July (Fig. 3b). For example, overall there was a 24% difference in average light and dark P_i-uptake rates in November (0.21 and 0.16 nmol P L^{-1} h^{-1}, respectively), and a 40% difference in July (0.89 and 0.53 nmol P L^{-1} h^{-1}, respectively).

3.3. Vertical profiles of DOP production

The short-term production of DOP also showed clear seasonal differences, with rates being low (<0.2 nmol P L^{-1} h^{-1}) in both November and July and higher (and more variable) in April (often >0.5 nmol P L^{-1} h^{-1}) (Fig. 4a). Production of DOP over the three sampling depths ranged from 0.07 to 0.39 nmol P L^{-1} h^{-1} in November, from 0.10 to 1.78 nmol P L^{-1} h^{-1} in April and from 0.02 to 0.24 nmol P L^{-1} h^{-1} in July. Hence, although DOP production was similar in November and July, it was slightly lower in July than November, and in April it varied from levels seen in the other months to values 5 to 7 times higher. In all three sampling periods, no variability in DOP production occurred in association with changes in the incubation irradiances (Fig. 4a): light-availability had no obvious influence on DOP production. Ratios of light to dark DOP production were mostly greater than 1 during all three sampling periods, with very few measurements showing ratios less than 1 (Fig. 4b). Light to dark DOP production ratios also showed no obvious variability in association with incubation irradiance.

Expressing DOP production as a fraction of total P_i-uptake (i.e. the sum of P_i-uptake and DOP production) shows clear patterns with sampling period and incubation irradiance (Fig. 4d). In November, the percentage extracellular release of DOP was consistently greater than 25% and increases up to 73% with decreasing incubation irradiance. A similar pattern was observed in April, although the levels of DOP release were slightly lower (down to 5-10% in some cases) (Fig. 4d). In contrast, DOP release in July was much lower (<20%) at all incubation irradiances, and in some cases DOP release in July was less than 5% of total P_i-uptake. Clearly, when P_i concentrations are at their lowest in July (<100 nmol P L^{-1}; Fig. 2a), DOP extracellular release (Figs. 4a and 4d) was at its lowest level, despite relatively high rates of P_i-uptake (Fig. 3a).

3.4. Integrated euphotic zone inventories

Nutrient concentrations and rates of P cycling were integrated across the euphotic layer for all 3 cruises (November, April and July), which we considered to roughly match the SML in November and early April, and then constrain both the SML and thermocline (and SCM) in late April and July (see Table 1). Rates of NPP, P_i-uptake and DOP release were scaled to daily integrals.

Euphotic zone integrals of Chl-*a* showed a clear seasonal progression of the phytoplankton communities, with average Chl-*a* concentrations highest in April (37.8-152.6 mg m^{-2}), intermediate in November (37.4-70.8 mg m^{-2}) and lowest in July (17.2-35.7 mg m^{-2}). Within April, Chl-*a* concentrations went from 49.6 mg m^{-2} in early April to a peak value of 152.6 mg m^{-2} in mid-April, which then decreased again towards the end of the month (Table 2). The mid-April Chl-*a* peak was associated with the spring bloom at the CCS site (Mayers et al., this issue) and discrete water-column Chl-*a* concentrations were as high as 8 mg m^{-3} (Fig. 2b). Increasing Chl-*a* concentrations throughout April were associated with a significant drawdown of P_i, as shown by declining P_i integrals from a high of 18.3 mmol P m^{-2} to values similar to those observed in November and July (i.e. <10 mmol P m^{-2}; Table 2). However, the depth distribution of P_i was drastically different between these two months (Fig. 2a): in November, moderate P_i concentrations (175-225 nmol P L^{-1}) occurred throughout the water-column, while in July P_i concentrations were extremely low (<100 nmol P L^{-1}) in the upper water-column and increased dramatically (up to 600 nmol P L^{-1}) in association with the nutricline (and SCM). Despite the presence of a SCM in July (Fig. 2b), this month had the lowest water-column inventories for Chl-*a* (Table 2).

As with Chl-*a* measurements, estimates of euphotic zone integrated phytoplankton biomass (C_{phyto}), based on conversion of cell counts, showed clear seasonal progression from low values in November and July to peak concentrations in April (Table 2). Generally, estimates of C_{phyto} were over 100 mmol C m^{-2} during April and less than 80 to 90 mmol C m^{-2} during the other sampling

periods. Estimated integrated bacteria biomass (C_{bact}) showed a similar seasonal pattern to C_{phyto}, relatively low and similar during November and July (ranges 24-32 and 23-33 mmol C m^{-2}, respectively) and peaking during April (27-182 mmol C m^{-2}) (Table 2). April was also associated with an increase over time at CCS from low C_{bact} (~50 mmol C m^{-2}) to high values around the peak in Chl-*a* around the latter half of the month (>140 mmol C m^{-2}). Ratios of C_{bact} to C_{phyto} (data not shown) were on average 0.34 (range 0.31-0.36) in November and 0.25 in July (0.17-0.37), and increased to an average of 0.48 (0.29-0.82) in April, again showing a temporal progression as the spring bloom peaked and nutrients declined.

Integrated net primary production (NPP) mirrored the seasonal changes in Chl-*a* concentrations, with rates low in November (average 32.4 mmol C m^{-2} d^{-1}) and July (average 35.4 mmol C m^{-2} d^{-1}), and peaking in mid-April at ~0.5 mol C m^{-2} d^{-1} (Table 2). As with Chl-*a*, April showed relatively low rates of NPP (<120 mmol C m^{-2} d^{-1}) early in the month, a peak on the 15th April and a decline to values roughly half of the peak (132-321 mmol C m^{-2} d^{-1}) at the end of the month. Clearly, the spring bloom in 2015 at CCS was associated with significant carbon fixation (see also Mayers et al., this issue). Normalising NPP to Chl-*a* concentrations shows a similar seasonal pattern in terms of the NPP per unit of phytoplankton biomass (Table 2). Integrated Chl-*a* normalised NPP rates were similar in November (average 0.7 gC (g Chl)$^{-1}$ h^{-1}) and July (average 1.1 gC (g Chl)$^{-1}$ h^{-1}), and peaked in mid-April with maximum values of 3.0 gC (g Chl)$^{-1}$ h^{-1} (average 2.0 gC (g Chl)$^{-1}$ h^{-1}) (Table 2). Such Chl-*a* normalised NPP rates indicate that phytoplankton communities in November and July were fixing (photosynthetically) around the same amount of C per gram of (Chl-*a*) biomass, while the community in April fixed almost double the amount for the same level of (Chl-*a*) biomass.

Euphotic zone integrals of POP showed a similar April peak to Chl-*a* and NPP, with the highest values in April (range 1.0 to 3.5 mmol P m^{-2}, average 2.3 mmol P m^{-2}), and with lower and more similar values in July (1.0-2.0 mmol P m^{-2}) and November (1.0-2.2 mmol P m^{-2}) (Table 2). Some of the highest integrated POP values (>3 mmol P m^{-2}) occurred in association with the high levels of Chl-*a* and NPP in mid-April at CCS. In contrast to POP (Chl-*a* and NPP), water-column integrated DOP concentrations showed a different seasonal pattern with values in November being the highest (11-25 mmol P m^{-2}), and with lower values in April (6-13 mmol P m^{-2}) and July (3-10 mmol P m^{-2}) (Table 2; see also Davis et al., this issue). In both April and July, integrated DOP concentrations were roughly equivalent to the size of the ambient P_i pool in the euphotic zone, while in November DOP concentrations were slightly higher than P_i. Though significant P_i drawdown was seen during April, there was no concurrent increase in the DOP pool, which only varied in size by ~6 to 7 mmol

510 P m^{-2} relative to a clear P_i drawdown of ~12 mmol P m^{-2} and a ~2 to 3 mmol P m^{-2} increase in POP
511 (Table 2).

512 The seasonal pattern of euphotic zone integrated P_i-uptake showed a peak in April (average 1.61
513 mmol P m^{-2} d^{-1}), with the July average roughly half of that in April (0.84 mmol P m^{-2} d^{-1}) and the
514 lowest rates (<0.30 mmol P m-2 d-1) in November (Table 2). The highest rate of integrated P_i-
515 uptake occurred in mid-April (2.08 mmol P m^{-2} d^{-1}) in association with the peak values of Chl-*a* and
516 NPP. However, unlike Chl-*a* and NPP, the P_i-uptake rates throughout April were much higher
517 (generally >1.3 mmol P m^{-2} d^{-1}) than those measured during the other sampling periods (range 0.14-
518 0.30 mmol P m^{-2} d^{-1} for November and 0.48-1.18 mmol P m^{-2} d^{-1} for July). In the case of integrated
519 DOP production (Table 2), the highest values occurred in April (average 0.49 mmol P m^{-2} d^{-1}), with
520 values in November ~3 times higher (average 0.17 mmol P m^{-2} d^{-1}) than those in July (average 0.05
521 mmol P m^{-2} d^{-1}). This pattern contrasts to that of the integrated P_i-uptake, with the highest DOP
522 production (>0.8 mmol P m^{-2} d^{-1}) occurring not in association with the peak in P_i-uptake, Chl-*a* or
523 NPP but rather 5 to 9 days later in April (Table 2). When integrated DOP production is expressed as
524 a fraction of total P_i-uptake (see Section 3.3) there are strong differences between the three
525 sampling periods (Table 2); DOP production represents (on average) a much higher fraction of total
526 P_i-uptake in November (41%) than in April (21%) or July (6%) (Table 2). The percentage
527 extracellular release of DOP was extremely low (<5%) in some cases in early July, with the low
528 values (<15%) seen in July only observed elsewhere during early April, well before the
529 development of the spring bloom and peak Chl-*a* around the 15th April.

530 **4. Discussion**

531 ***4.1. The dynamics of Phosphate uptake***

532 The uptake of nutrients (N, P) and photosynthetic C-fixation, and the resulting stoichiometric
533 balance of cellular constituents vary on timescales from almost instantaneous to daily adjustments
534 (e.g., Geider and La Roche, 2002; Rees et al., 1999; Talmy et al., 2014; Lopez et al., 2016).
535 Ecological interactions also occur across various timescales, resulting in stoichiometric balances
536 that vary in time and space, with important implications for the biogeochemistry of marine
537 ecosystems (Sterner and Elser, 2002). Short-term measurements need to be scaled to the appropriate
538 integrated time- and depth-scales (e.g. daily, euphotic zone), and with clear perspectives on what is
539 (or is not) measured is required prior to examining system-scale biogeochemical processes.

540 The potentially rapid recycling of P leads to the requirement that uptake (and release) measurements
541 are considered over short-time periods, whereas photosynthetic C-fixation occurs throughout the
542 (seasonally variable) daylight period. Short-term P_i-uptake measurements are often scaled to a 24 h

period, with the inherent assumption that uptake rates are temporally invariable. To examine this, we undertook two time-series incubations of P_i-uptake, with measurements every 4 h over a period of 24 h (Fig. 5). One time-series incubation began at 6 am (local time) on the 17th July and the second at 9 am (local time) on the 23rd July, with both experiments showing a steady increase in P_i-uptake prior to sunset and then a slight decline during the night (Fig. 5a). Average P_i-uptake (± S.D.) for these incubations was 0.72 ± 0.20 and 0.92 ± 0.22 nmol P L^{-1} h^{-1}, respectively, which are higher than the initial 4 h measurements (0.43 ± 0.06 and 0.67 ± 0.08 nmol P L^{-1} h^{-1}, respectively). If the initial measurements are scaled by 24 h, daily rates of 9.6 nmol P L^{-1} d^{-1} and 16.8 nmol P L^{-1} d^{-1} are calculated, which are 26 to 47% less than the cumulative 24 h rates (Fig. 5b). These results caution that short-term rates of P_i-uptake may vary during day- and night-time periods, and hence scaling these initial rates may result in a significant underestimation of daily P_i-uptake.

However, these results should also be viewed cautiously, as they represent only two time-series of P_i-uptake, when P_i concentrations were at their lowest seasonal level (Table 1). Further time-series of P_i-uptake need to be considered in the context of diurnal changes in cellular metabolism, and between different components of the plankton (bacteria, phytoplankton). Interpretation of diurnal changes in P_i-uptake may also be complicated if, for example, P_i concentrations and biomass are not constant in the incubations (neither of which were measured in our experiments). Though we acknowledge that short-term P_i-uptake measurements may not simply scale with day length (Fig. 5), to make our observations consistent with the existing literature (e.g., Reynolds et al., 2014) we have retained simple scaling to day lengths. Furthermore, the focus of the present study was to examine seasonal (inter-cruise) differences in P_i-uptake and such overestimates may be systematic for each sampling period.

Both bacteria and phytoplankton are involved in P uptake in marine systems (Popendorf and Duhamel, 2015), with phytoplankton P_i-uptake related to some extent by light availability whilst bacterial uptake may be unrelated to light level. Across all three seasonal sampling periods, rates of both P_i-uptake and DOP production in light-exposed (L) incubations were higher than those incubated in the dark (D), with L:D ratios consistently greater than 1 (Figs. 3b and 4b). For P_i-uptake, L:D ratios were greater than 1.5 at the highest incubation irradiances (>0.6 mol quanta m^{-2} h^{-1}) in November and April, and across most of the light gradient in July. Light availability clearly enhanced P_i-uptake, which may be analogous to the reduced rates of P_i-uptake during the night-time time-series experiments (Fig. 5a).

In the case of DOP production, L:D ratios were also slightly higher than 1 during July, and in general the L:D ratios were similar in magnitude and trend to those seen in P_i-uptake (Fig. 4b): hence the irradiance-influence on P_i-uptake was mirrored in the subsequent release of DOP, though

the relative percentage extracellular release of DOP differed seasonally (Fig. 4d). Ratios of L:D P_i-uptake in other studies have also been found to be greater than 1, for example in the North Atlantic (Donald et al., 2001) and Pacific Ocean (Duhamel et al., 2012), although ratios closer to 1 have been reported from the North Pacific subtropical gyre (Björkman et al. 2000). Variability in L:D uptake ratios likely reflects the relative contribution of phytoplankton and bacteria, as well as seasonal variability in substrate (P_i) availability and energetic (light, C) constraints on P_i-uptake and cellular P-demands (Sterner and Elser, 2002; Björkman et al., 2000).

Competition between bacteria and phytoplankton for P is a strong driver of biogeochemistry in marine ecosystems (Thingstad et al., 1993, 1996; Popendorf and Duhamel, 2015). Previous studies of planktonic P_i-uptake have shown differentiated bacterial and algal P-uptake using different pore-sized filters, for example considering bacterial uptake as from cells less than 0.6 µm and algal uptake from cells greater than 0.6 µm (e.g., Duhamel and Moutin, 2009). However, both bacterial and algal cell sizes are variable with taxonomy and physiological status and may overlap in size-distribution; for example, the cyanobacteria *Synechococcus*, which is numerically dominant in the Celtic Sea in summer (Hickman et al., 2012), and ranges in cell size in association with growth rate and nutrient conditions (Lopez et al., 2016). In this study, 0.45 µm filters were used to ensure that P_i-uptake from *Synechococcus* was fully included in our measurements at the same time as (partly) excluding the influence of heterotrophic bacteria.

To test this assumption, size-fractionation experiments were performed during summer with samples size-fractionated (0.2, 0.45, 0.8 and 2 µm) post-incubation to determine the P_i-uptake by different fractions (Supplementary Fig. S1). These experiments indicated that the 0.45 µm P_i-uptake represented on average 55% (range 32-84%) of the total (0.2 µm) P_i-uptake, while the 0.8 µm fraction represented 36% (19-42%), and the greater than 2 µm fraction 14% (10-19%). These differential contributions are similar to those found by Duhamel and Moutin (2009) (~15-43% 0.2-0.6 µm, ~20-75% 0.6-2 µm, ~10-50% >2 µm), implying that although the use of 0.45 µm filters removed a proportion of bacterial P_i-uptake (0.2-0.45 µm), our measurements of P_i-uptake may not be exclusively from phytoplankton and likely include some bacterial P_i-uptake. Hence, when considering the P-dynamics observed seasonally the composition of the plankton community in terms of both phytoplankton and bacteria needs to be considered.

4.2. Seasonal changes in Phosphate uptake and DOP release in the Celtic Sea

Observations from November to July in the Celtic Sea showed clear seasonal patterns in plankton community composition (Mayers et al., this issue; Giering et al., this issue) and biogeochemical processes (Garcia-Martin et al., this issue-A & B). Phytoplankton biomass (Chl-*a* and C_{phyto}) and

NPP both peaked in April and diverged in November and July, with Chl-*a* levels halved in July relative to November, although levels of C_{phyto} and NPP were more similar (Tables 1 and 2). This divergence is linked to seasonality in C to Chl-*a* ratios at CCS; using the cruise average values for C_{phyto} and Chl-*a* from Table 2, we calculated C:Chl-*a* ratios (g:g) of 16 for November, 26 for April and 53 for July. Such estimates are similar to those made by Holligan et al. (1984) for summer in the Celtic Sea, and are driven by cellular responses to seasonal variability in resource (light, nutrients) availability (Geider, 1987; Artega et al., 2016).

Seasonality in C:Chl-*a* ratios in the Celtic Sea link to variability in P_i (and NO_x) concentrations and average surface mixed layer irradiances ($\bar{E}_{SML}$; Table 1); with low $\bar{E}_{SML}$ and high P_i in November and high $\bar{E}_{SML}$ and low P_i in July. Phytoplankton dynamics in autumn may be considered light-driven while summer was nutrient-driven, with spring a transition between these two. Light levels ($\bar{E}_{SML}$) in November were low (average: 1.9 mol quanta m^{-2} d^{-1}, Table 1), only slightly above the critical compensation irradiance for net growth in North Atlantic phytoplankton communities (1.3 mol quanta m^{-2} d^{-1}, Siegel et al., 2002), and lower than levels suggested to limit Southern Ocean communities (3 mol quanta m^{-2} d^{-1}, Venables and Moore, 2010). Nitrogen (nitrate, NO_x) availability has been proposed previously to limit primary production during summer in the Celtic Sea (Pemberton et al., 2004; Davis et al., 2014). Low N* values seen at CCS support such a conclusion, along with depletion of NO_x below detection levels (<20 nM) in July whilst P_i remained above 55 nM (Table 1).

As well as phytoplankton biomass (Chl-*a*, C_{phyto}) and NPP, particulate organic phosphorus (POP) also peaked in April (average: 2.3 mmol P m^{-2}) whilst concentrations in November and July were relatively similar (1.4 and 1.5 mmol P m^{-2}, respectively) (Table 2). Cruise averages (and ranges) for euphotic zone integrated DOP concentrations (Table 2) were twice as high in November (11-25 mmol P m^{-2}) relative to April (6-13 mmol P m^{-2}) and July (3-10 mmol P m^{-2}), with the summer values the lowest overall. This is the same pattern as seen by Davis et al. (this issue) for the SML in the Celtic Sea from a larger number of stations, with summer conditions also associated with the lowest water-column (0-150 m) integrated DOP. Lower DOP concentrations in summer are likely to be associated with the lower production rates (Fig. 4a, Table 2) and advective losses, as well as the possible utilization of DOP (see Davis et al., this issue), which may occur in severely P-stressed conditions (Dyhram and Ruttenberg, 2006; Dyhram et al., 2007; Duhamel et al., 2014). Summation of the different P pools (P_i, POP and DOP) at CCS shows only a slight decline in the total P pool over time (averages: 29.4 to 24.2 mmol P m^{-2} from November to April, down to 12.2 mmol P m^{-2} in July). The proportion of total P in the DOP and P_i pools remained 45 to 56% and 34 to 39%, respectively, while the fraction in the POP pool increased slightly from 5% in autumn to 14% in

summer (data not shown). Hence, there was a loss of P from the euphotic zone that may have been linked to the sinking of particulate material below the thermocline and/or the advection of semi-labile DOP (Reynolds et al., 2014; Davis et al., this issue).

April was also associated with a peak in P_i-uptake, with rates in July four times higher than those in November, despite the reduced nutrient concentrations and P_i pool size (Tables 1 and 2). The affinity of the plankton community for P_i-uptake can be assessed by examining the biomass-specific turnover rate ($1/P_i$ turnover × POP), where biomass is represented by POP and the units are proportional to the volume of water cleared of substrate per unit biomass per unit time (Thingstad and Rassoulzadegan, 1999; Tambi et al., 2009). For CCS, average values calculated this way for November were 1.1 L pmol P^{-1} h^{-1} and were 5-times higher in April (5.4 L pmol P^{-1} h^{-1}) and 10-times higher in July (11.1 L pmol P^{-1} h^{-1}); indicating that the affinity for P_i-uptake was highest in summer rather than spring. The amount of this P_i taken up by the plankton that was then released as DOP varied considerably between April and July, with the percentage extracellular release of DOP highest in November (31-58%), then declining in April (7-45%) to a minimum in July (2-11%) (Table 2).

To conclude, the summertime planktonic ecosystem in the Celtic Sea was highly efficient at P_i-uptake and P-retention when P_i concentrations were low, and N-availability limited ecosystem productivity. Such a system, with a high biomass-normalised affinity for P_i-uptake, had high rates of recycling supporting relatively high rates of NPP (and P_i-uptake). Rates of NPP in summer were also supported by regenerated sources of N rather than inorganic forms (Humphreys et al., this issue). In contrast, the autumn ecosystem was the least efficient at P_i-uptake or P-retention, with light as the most likely limiting factor for this community. In autumn, P_i-concentrations were also relatively high and sufficient to support the low rates of NPP and P_i-uptake observed, with a potentially light-limited system with a low affinity for P-cycling. Spring was a transitional period, with the ecosystem evolving from a light-limited system as the water-column stratified and rates of P_i-uptake and DOP production increased. The latter half of spring differs from the summer, as despite the decline in P_i concentrations, P-retention remained low whilst summer conditions were associated with efficient P-retention. The later stages of the spring bloom does not appear to be characterised by well-developed P-recycling mechanisms, and DOP production may be driven by high mortality related losses due to zooplankton (Mayers et al., this issue).

4.3. Seasonal changes in the turnover of the different P pools in the Celtic Sea

Consideration of pool sizes and uptake rates only gives limited insights into biogeochemical processes. Rather, consideration of the turnover rates of the different pools accounts for both the

677 relative pool size and uptake rate, providing further information on the dynamics of the system
678 (Benitez-Nelson, 2000). Short turnover times (a few hours or days) implies rapid biological
679 utilization, whilst longer turnover times (weeks or longer) indicate a lack of bioavailability or lower
680 requirements (Benitez-Nelson, 2000). Comparison of turnover times of related pools (e.g., C_{phyto}
681 and POC; Poulton et al., 2006) may also provide further insights into underlying ecological and
682 biogeochemical processes.

683 Phytoplankton turnover times, calculated from C_{phyto} and NPP (following Leynaert et al., 2000; see
684 also Poulton et al., 2006), show strong seasonality with short turnover times (<1 day) in April
685 compared with longer turnover times in both November and July (1.5-2.2 d and 1.1-4.4 d,
686 respectively) (Table 3). This seasonality in phytoplankton turnover times supports the suggestion of
687 light-limited growth in autumn and nutrient-stress in summer, as well as the rapid development of
688 the spring bloom through April (Table 2; see also Mayers et al., this issue; Garcia-Martin et al., this
689 issue-B). Inefficient utilization of the P_i pool in autumn relative to efficient utilization in spring and
690 summer is also supported by the seasonal differences in turnover times of this pool; from 21.9 to
691 42.3 d in November to 2.7 to 8.8 d in July, with turnover times in April declining from 8.9 d to 2.2
692 d (Table 3).

693 Turnover of the POP pool was slowest in November (2.8-4.9 d), with slightly faster turnover of
694 C_{phyto} (average 1.7 d) relative to POP (average 3.9 d), which may be indicative of plankton other
695 than phytoplankton (i.e., heterotrophic bacteria) strongly contributing to the POP pool. The
696 relatively rapid turnover of P_i and POP during summer and late spring, when P_i concentrations were
697 depleted (<10 mmol P m^{-2}; Table 2), also implies efficient P-recycling (Benitez-Nelson and
698 Buesseler, 1999), even though these turnover times are longer than the very rapid turnover (<1 d)
699 observed in P-limited open-ocean regions (e.g., Sohm and Capone, 2010). This efficient P-recycling
700 in the Celtic Sea during summer, as well as utilisation of regenerated forms of N (Humphreys et al.,
701 this issue), supported similar levels of NPP to autumn, as well as relatively high rates of P_i-uptake
702 despite the seasonal differences in P_i availability (Table 2).

703 Turnover times for POP in April and July were surprisingly similar (0.5-1.3 d and 1.0-1.4 d,
704 respectively) when considering the much longer C_{phyto} turnover times in July (1.1-4.4 d; Table 3).
705 One interpretation of this discrepancy is that the two pools were composed of different components
706 during July, for example a greater heterotrophic bacterial contribution (or activity) in July than
707 November or April. Estimates of euphotic zone integrated bacterial biomass (C_{bact}; Table 2) were
708 very similar in autumn and summer, and highest in spring. However, bacterial growth efficiency,
709 due to low respiratory C-losses and high C-fixation, were highest in July (61 ± 5%) rather than in
710 November (27 ± 3%) or April (36 ± 6%) (Garcia-Martin et al., this issue-A). Though summer C_{bact}

was similar to levels seen in autumn (and lower than in spring), its turnover time was much shorter in summer; combining average values of bacterial production (see Garcia-Martin et al. this issue-A) with average integrated bacterial biomass (Table 2) gives turnover times of 1.2 d in July, 4.7 d in November and 5.6 d in April. These C_{bact} turnover times are similar to those for the POP pool in both July and November (1.1 d and 3.9 d, respectively), but not in April (0.9 d) (Table 3). These similarities likely indicate a significant bacterial contribution to both P_i-uptake rates and the POP pool in summer and autumn. Though C_{bact} increased relative to C_{phyto} in spring (Table 2), bacterial production remained low due to low growth efficiencies (Garcia-Martin et al., this issue-A), suggesting that bacteria had less influence on P_i-uptake in spring than in autumn or summer.

The turnover times for the DOP pool were much longer (>40 d) than those for the other pools (Table 3), although much shorter turnover (<10 d) did occur during late April. Slow turnover of DOP in November was driven by relatively high DOP concentrations (11-25 mmol P m^{-2}) and moderate DOP production (0.11-0.28 mmol P m^{-2} d^{-1}), although this sampling period also had the highest overall relative percentage extracellular release (31-58%) (Table 3). July had similar slow rates of DOP turnover to November (Table 3), although lower DOP concentrations and DOP production rates (and the lowest overall extracellular release, ranging from 2-11%) (Table 2). Hence, during both autumn and summer the DOP pool was largely inactive, with a large pool size relative to low rates of DOP production. A contrasting situation was found in the Celtic Sea during spring, especially during the latter half of the bloom where concentrations of P_i declined below 10 mmol P m^{-2} (<200 nmol P L^{-1}) and DOP production rates increased above ~0.5 mmol P m^{-2} d^{-1} (Tables 1 and 2). Relatively short turnover times (range 4-17 d; Table 3) during the latter half of April could potentially indicate a degree of DOP utilization by the plankton community during the latter stages of the spring bloom, as inorganic nutrient sources declined (and both C_{phyto} and C_{bact} increased; Table 2), and where the bioavailability of DOP may have increased (see Björkman et al., 2000; Björkman and Karl, 2003).

The turnover times of the different C and P pools in the Celtic Sea provide support to the suggestions of seasonal patterns in resource availability and their influence on P dynamics. Slow P_i turnover in autumn was caused by the low-affinity ecosystem present, with inefficient P-dynamics driven by light-limitation. In spring and summer, P_i availability became increasingly important with a succession to a summer-time high-affinity ecosystem and efficient P dynamics. Summer was also potentially associated with a strong bacterial influence on P dynamics. DOP turnover was relatively slow throughout spring, summer and fall, indicating little biological utilization of this P-pool. The lack of accumulation of DOP during summer contrasts with a previous Celtic Sea study by Davis et al. (2014), potentially due to the low production rates observed in summer in this study.

4.4. Seasonality in particulate stoichiometry in the Celtic Sea

The last two sections have highlighted how seasonal variability in P_i-uptake and P-retention in the Celtic Sea is related to both the composition of the plankton community (C_{phyto}, C_{bact}) and resource (P_i, light) availability. Light-limitation led to an ecosystem composed of slow growing phytoplankton and bacteria with inefficient P_i-uptake or P-retention. Low nutrient concentrations (P_i, NO_x) in summer led to an efficient recycling ecosystem with slow-growing phytoplankton and fast-growing bacteria influencing both high P_i-uptake and low DOP production. The spring bloom was transitional between these two situations, with fast growing phytoplankton dominating P_i-uptake and increasing DOP production as nutrient availability declined (P_i, NO_x). Such seasonal variability in P_i-uptake, DOP production, plankton composition and NPP (C-fixation) will all result in variability in the stoichiometric ratio of planktonic C to P uptake.

Taking the ratio of NPP to P_i-uptake (mol:mol) as indicative of the planktonic C:P (i.e. DIC:P_i) uptake ratio shows clear seasonality (Table 3). Average ratios of NPP:P_i-uptake for each sampling period ranged from 132 (range: 75-188) in November, to 116 (54-256) in April and 44 (21-53) in July. Relative to the Redfield ratio (106:1), these ratios indicate a seasonal transition from slightly C-rich uptake in autumn (and late spring) to strongly P-rich uptake in summer (and early spring) (Table 3). If total P_i-uptake (i.e., tP_i = P_i-uptake + DOP production) is considered, then the relatively high percentage extracellular release of DOP during autumn and late spring lead to C:P ratios which are strongly P-rich relative to the Redfield ratio; with cruise averages of 81 (range: 37-123) in November, 90 (46-195) in April and 42 (20-68) in July (Table 3). However, whether net or total P_i-uptake are considered, autumn and spring are still, on average, more C-rich in their uptake rates than summer, which was more P-rich.

In autumn, NPP:P_i-uptake ratios close to (and slightly higher) than the Redfield ratio were associated with an ecosystem which was potentially light-limited, with low rates of NPP and P_i-uptake, high DOP production and, though growing slowly, a bacterial influence. The spring bloom was associated with a transition from light-limitation to low nutrient conditions as P_i concentrations declined, with rapid phytoplankton turnover times (i.e., fast growth rates) slowing as resource availability declined. NPP increased to a peak in spring and then declined slightly with nutrient concentrations, whereas P_i-uptake remained high despite the decline in nutrient concentrations (Tables 1 and 2). The ratio of NPP:P_i-uptake was low (P-rich) during early spring in association with rapid phytoplankton growth rates, as is expected in nutrient-replete and optimal growth conditions (Sterner and Elser, 2002), and then the ratio increased (C-rich) as growth slowed and nutrient levels declined (Tables 2 and 3). This pattern in C:P uptake stoichiometry, from P-rich organic matter formation in early spring to C-rich production in late spring, agrees well with

Humphreys et al. (this issue), who came to the same conclusion based on nutrient and dissolved inorganic carbon dynamics during April.

The low NPP:P_i-uptake ratios (P-rich) in summer were not associated with rapid phytoplankton growth (Table 3), but rather with high bacterial growth rates and a stronger bacterial influence on C:P uptake (and retention). Heterotrophic bacteria are recognised as strong competitors for P_i under nutrient depleted conditions (Thingstad et al., 1993, 1996; Duhamel and Moutin, 2009). Whilst phytoplankton cellular C:P stoichiometry is near, or slightly lower, than the Redfield ratio (Geider and LaRoche, 2002; Ho et al., 2003), bacterial cellular C:P ratios are significantly more P-rich (e.g., ~50; Fagerbakke et al., 1996; Sterner and Elser, 2002; Hessen et al., 2004; Duhamel and Moutin, 2009; see also Scott et al., 2012). Thus, it is suggested that the relatively P-rich uptake ratios in summer relate to a stronger bacterial influence on P_i-uptake through increased competition as P_i availability was low, bacterial growth efficiency was high (Garcia-Martin et al., this issue-A) and phytoplankton growth rates were relatively low.

4.5. Implications for the Continental Shelf Pump

When considering the Continental Shelf Pump (CSP), C-overconsumption relative to nutrient utilization (N, P) is an important factor in regulating the magnitude and efficiency of the CSP. Such C-overconsumption has been suggested to occur during the nutrient-impoverished summer period, when nutrient-starved phytoplankton may have high cellular C:P and excrete C-rich dissolved organic matter (Toggweiler et al., 1993; Thomas et al., 2004, 2005; Bozec et al., 2006; Kühn et al., 2010). In the Celtic Sea, Davis et al. (this issue) observed that both the particulate and dissolved pools showed seasonal succession in becoming increasingly C-rich relative to the Redfield ratio from autumn through spring and into summer. In this context, our observations of P-rich uptake in July may appear paradoxical, however what they imply is that significantly more C-rich biogeochemical processes must be balancing out the influence of plankton uptake stoichiometry on particulate and dissolved organic matter stoichiometry.

In the case of particulate material in summer, when bacteria appear to dominate P-uptake and retention, other components of the plankton (phytoplankton, zooplankton), as well as detrital material, may all be relatively C-rich. Slow-growing phytoplankton in summer (Table 3) still represented more biomass than bacteria (C_{bact}:C_{phyto} ~0.17-0.37) and hence may be more influential on particulate stoichiometry than nutrient recycling. For the dissolved pool in summer, the plankton community may excrete large quantities of dissolved organic carbon (see Garcia-Martin et al., this issue A), whereas our observations indicate that they are releasing very little in terms of DOP. Hence, the dissolved organic matter pool in summer will become strongly enriched in C, with

results from Davis et al. (this issue) showing the summertime DOM pool had C:P ratios 3 times higher than the Redfield ratio (see also Humphreys et al., this issue). Overall, our results have two important implications for the CSP: 1) both autotrophs and heterotrophs seasonally influence nutrient (P, N) recycling and uptake (C:P) stoichiometry, and 2) there is a tendency for uptake (C:P) stoichiometry to be nutrient-rich rather than strongly C-rich, as would be expected to support an efficient CSP. Hence, for a nutrient-efficient CSP (and C-overconsumption), other biogeochemical processes involved (e.g. DOM production, particulate remineralisation) need to be relatively C-rich to balance out the influence of uptake stoichiometry.

5. Conclusions

In this study, seasonal variability in P_i-uptake and DOP production in the Celtic Sea was related to both the composition of the plankton community (C_{phyto}, C_{bact}) and resource (P_i, light, NO_x) availability. In autumn, light-limitation led to an ecosystem composed of slow-growing phytoplankton and bacteria with relatively low P_i-uptake and with high DOP production. In summer, low nutrients (low P_i, depleted NO_x) led to an efficient recycling ecosystem supporting relatively high NPP with slow-growing phytoplankton, and fast-growing bacteria influencing high P_i-uptake and low DOP production. The spring bloom in the Celtic Sea was transitional between these two situations, with fast-growing phytoplankton dominating P_i-uptake with increasing DOP production (in absolute and relative terms) as inorganic nutrients declined (P_i, NO_x) towards the latter stages of the bloom.

These seasonal changes in ecosystem dynamics were associated with changes in the ratio of C to P uptake, as described by the ratio of NPP to P_i-uptake in this study, with the summer relatively more P-rich in terms of uptake than autumn or spring. Such P-rich uptake was associated with a stronger influence of actively growing heterotrophic bacteria rather than phytoplankton activity, whereas P-rich uptake in early spring was associated with fast phytoplankton growth in optimal growth (bloom) conditions. In terms of our original hypotheses, P-rich uptake associated with fast phytoplankton growth in the spring bloom goes against the first hypothesis (i.e. that optimal growth conditions in spring would lead to uptake stoichiometry in Redfield proportions), and rather supports the ‘growth-rate hypothesis’ of Sterner and Elser (2002). Whilst departures from the Redfield ratio in uptake stoichiometry did occur in response to changes in resource (light, nutrients) availability (the second hypothesis), such departures were also associated with different seasonal influences of autotrophs and heterotrophs. Hence, our results highlight the importance of considering the full plankton community in terms of seasonal P-dynamics, and in the underlying mechanisms supporting the CSP.

Acknowledgements

The authors would like to acknowledge the support of the captains, officers and crews of the associated Shelf Sea Biogeochemistry cruises, as well as J. Sharples and M. Moore who acted as the Principal Scientific Officers for the November and July cruises. This study was supported by the UK Natural Environmental Research Council via the Shelf Sea Biogeochemistry research programme, through grants NE/K001701/1, NE/K002007/1 and NE/K002058/1. KM was supported by a NERC Doctoral Training Partnership (DTP) studentship as part of the Southampton Partnership for Innovative Training of Future Investigators Researching the Environment (SPITFIRE).

References

Arrigo, K.R., 2005. Marine microorganisms and global nutrient cycles. Nature 437, doi: 10.1038/nature04159.

Arteaga, L., Pahlow, M., Oschlies, A., 2016. Modeled Chl:C ratio and derived estimates of phytoplankton carbon biomass and its contribution to total particulate organic carbon in the global surface ocean. Global Biogeochemical Cycles, 30, doi: 10.1002/2016GB005458.

Bauer, J.E., Cai, W-J., Raymond, P.A., Bianchi, T.S., Hopkinson, C.S., Regnier, P.A.G., 2013. The changing carbon cycle of the coastal ocean. Nature Geoscience 504, 61-70.

Benitez-Nelson, C.R., 2000. The biogeochemical cycling of phosphorus in marine systems. Earth-Science Reviews 51, 109-135.

Benitez-Nelson, C.R., Buesseler, K.O., 1999. Variability in inorganic and organic phosphorus turnover rates in the coastal ocean. Nature 398, 502-505.

Björkman, K.M., Thomson-Bulldis, A.L., Karl, D.M., 2000. Phosphorus dynamics in the North Pacific subtropical gyre. Marine Ecology Progress Series 22, 185-198.

Björkman, K.M., Karl, D.M., 2003. Bioavailability of dissolved organic phosphorus in the euphotic zone at Station ALOHA, North Pacific Subtropical Gyre. Limnology and Oceanography 48, 1049-1057.

Bozec, Y., Thomas, H., Schiettecatte, L-S., Borges, A.V., Elkalay, K., de Baar, H.J.W., 2006. Assessment of the processes controlling seasonal variations of dissolved inorganic carbon in the North Sea. Limnology and Oceanography 51, 2746-2762.

Burkhardt, B.G., Watkins-Brandt, K.S., Defforey, D., Paytan, A., White, A.E., 2014. Remineralization of phytoplankton-derived organic matter by natural populations of heterotrophic bacteria. Marine Chemistry 163, 1-9.

877 Davis, C.E., Mahaffey, C., Wolff, G.A., Sharples, J., 2014. A storm in a shelf sea: Variability in
878 phosphorus distribution and organic matter stoichiometry. Geophysical Research Letters 41, doi:
879 10.1002/2014GL061949.
880 Davis, C.E., Blackbird, S., Wolff, G.A., Sharples, J., Woodward, E.M.S., Mahaffey, C. Seasonal
881 organic matter dynamics in a temperate shelf sea. Progress in Oceanography, this issue.
882 Donald, K.M., Joint, I., Rees, A.P., Woodward, E.M.S., Savidge, G., 2001. Uptake of carbon,
883 nitrogen and phosphorus by phytoplankton along the 20^{o}W meridian in the NE Atlantic between
884 57.5^{o}N and 37^{o}N. Deep-Sea Research II 48, 873-897.
885 Duhamel, S., Moutin, T., 2009. Carbon and phosphate incorporation rates of microbial assemblages
886 in contrasting environments in the Southeast Pacific. Marine Ecology Progress Series 375, 53-
887 64.
888 Duhamel, S., Björkman, K.M., Karl, D.M., 2012. Light dependence of phosphorus uptake by
889 microorganisms in the subtropical North and South Pacific Ocean. Aquatic Microbial Ecology
890 67, 225-238.
891 Duhamel, S., Björkman, K.M., Doggett, J.K., Karl, D.M., 2014. Microbial response to enhanced
892 phosphorus cycling in the North Pacific Subtropical Gyre. Marine Ecology Progress Series 504,
893 43-58.
894 Dyhrman, S.T., Ammerman, J.W., Van Mooy, B.A.S., 2007. Microbes and the marine phosphorus
895 cycle. Oceanography 20, 110-116.
896 Dyhrman, S.T., Ruttenberg, K.C., 2006. Presence and regulation of alkaline phosphatase activity in
897 eukaryotic phytoplankton from the coastal ocean: Implications for dissolved organic phosphorus
898 remineralization. Limnology and Oceanography 51, 1381-1390.
899 Elser, J.J., Kyle, M., Makino, W., Yoshida, T., Urabe, J., 2003. Ecological stoichiometry in the
900 microbial food web: a test of the light: nutrient hypothesis. Aquatic Microbial Ecology 31, 49-
901 65.
902 Faggerbakke, K.M., Heldal, M., Norland, S., 1996. Content of carbon, nitrogen, oxygen, sulfur and
903 phosphorus in native aquatic and cultured bacteria. Aquatic Microbial Ecology 10, 15-27.
904 Falkowski, P.G., 2000. Rationalizing elemental ratios in unicellular algae. Journal of Phycology 36,
905 3-6.
906 Falkowski, P.G., Davis, C.S., 2004. Natural proportions. Nature 431, 131.
907 Finkel, Z.V., Beardall, J., Flynn, K.J., Quigg, A., Rees, T.A.V., Raven, J.A., 2010. Phytoplankton in
908 a changing world: cell size and elemental stoichiometry. Journal of Plankton Research 32, 119-
909 137.
910 García-Martín, E.E., Daniels, C.J., Davidson, K., Davis, C.E., Mahaffey, C., Mayers, K.M.J.,
911 McNeil, S., Poulton, A.J., Purdie, D.A., Tarran, G., Robinson, C. Seasonal changes in

912 microplankton respiration and bacterial metabolism in a temperate Shelf Sea. Progress in
913 Oceanography, this issue-A.
914 García-Martín, E.E., Daniels, C.J., Davidson, K., Lozano, J., Mayers, K.M.J., McNeil, S., Mitchell,
915 E., Poulton, A.J., Purdie, D.A., Tarran, G., Whyte, C., Robinson, C. Plankton community
916 respiration and bacterial metabolism in a North Atlantic shelf sea during spring bloom
917 development (April 2015). Progress in Oceanography, this issue-B.
918 Geider, R., 1987. Light and temperature dependence of the carbon to chlorophyll-a ratio in
919 microalgae and cyanobacteria: implications for physiology and growth of phytoplankton. New
920 Phytologist 106, 1-34.
921 Geider, R., La Roche, J., 2002. Redfield revisited: variability of C:N:P in marine microalgae and its
922 biochemical basis. European Journal of Phycology 37, 1-17.
923 Giering, S.L.C., Wells, S.R., Mayers, K.M.J., Schuster, H., Cornwell, L., Fileman, E., Atkinson, A.,
924 Cook, K.B., Preece, C., Mayor, D.J. Seasonal variation of zooplankton community structure and
925 trophic position in the Celtic Sea: a stable isotope and biovolume spectrum approach. Progress in
926 Oceanography, this issue.
927 Hessen, D.O., Færøvig, P.J., Andersen, T., 2002. Light, nutrients, and P:C ratios in algae: Grazer
928 performance related to food quality and quantity. Ecology 83, 1886-1898.
929 Hessen, D.O., Ågren, G.I., Anderson, T.R., Elser, J.T., de Ruiter, P.C., 2004. Carbon sequestration
930 in ecosystems: The role of stoichiometry. Ecology 85, 1179-1192.
931 Hickman, A.E., Moore, C.M., Sharples, J., Lucas, M.I., Tilstone, G.H., Krivtsov, V., Holligan,
932 P.M., 2012. Primary production and nitrate uptake within the seasonal thermocline of a stratified
933 shelf sea. Marine Ecology Progress Series 463, 39-57.
934 Ho, T-Y., Quigg, A., Finkel, Z.V., Milligan, A.J., Wyman, K., Falkowski, P.G., Morel, F.M.M.,
935 2003. The elemental composition of some marine phytoplankton. Journal of Phycology 39,
936 1145-1159.
937 Holligan, P.M., Harris, R.P., Newe, R.C., Harbour, D.S., Head, R.N., 1984. Vertical distribution
938 and partitioning of organic carbon in mixed, frontal and stratified waters of the English Channel.
939 Marine Ecology Progress Series 14, 111-127.
940 Humphreys, M.P., Achterberg, E.P., Chowdhury, M.Z.H., Griffiths, A.M., Hartman, S.E., Hopkins,
941 J.E., Hull, T., Kivimae, C., Smilenova, A., Wihsgott, J., Woodward, E.M.S., Moore, C.M.
942 Mechanisms for a nutrient-conserving carbon pump in a seasonally stratified, temperate
943 continental shelf sea. Progress in Oceanography, this issue.
944 Hydes, D.J., Aoyama, M., Aminot, A., Bakker, K., Becker, S., Coverly, S., Daniel, A., Dickson,
945 A.G., Grosso, O., Kerouel, R., van Ooijen, J., Sato, K., Tanhua, T., Woodward, E.M.S., Zhang,
946 J.Z., 2010. Determination of dissolved nutrients (N, P, Si) in seawater with high precision and

947 inter-comparability using gas-segmented continuous flow analysers. In: The GO-SHIP repeat
948 hydrography manual: A collection of expert reports and guidelines. IOCCP report No. 14, ICPO
949 publication series No. 134.
950 Joint, I., Wollast, R., Chou, L., Batten, S., Elskens, M., Edwards, E., Hirst, A., Burkill, P., Groom ,
951 S., Gibb, S., Miller, A., Hydes, D., Dehairs, F., Antia, A., Barlow, R., Rees, A., Pomroy, A.,
952 Brockmann, U., Cummings, D., Lampitt, R., Loijens, M., Mantoura, F., Miller, P., Raabe, T.,
953 Alvarez-Salgado, X., Stelfox, C., Woolfenden, J., 2001. Pelagic production at the Celtic Sea
954 shelf break. Deep-Sea Research Part II 48, 14-15.
955 Karl, D.M., 2000. Phosphorus, the staff of life. Nature 406, 31-33.
956 Karl, D.M., Tien, G., 1992. MAGIC: A sensitive and precise method for measuring dissolved
957 phosphorus in aquatic environments. Limnology and Oceanography 37, 103-116.
958 Karl, D.M., Björkman, K.M., Dore, J.E., Fujieki, L., Hebel, D.V., Houlihan, T., Letelier, R.M.,
959 Tupas, L.M., 2001. Ecological nitrogen-to-phosphorus stoichiometry at station ALOHA. Deep
960 Sea Research II 48, 1529-1566.
961 Kovala, P.E., Larrence, J.D., 1966. Computation of phytoplankton number, cell volume, cell surface
962 and plasma volume per litre, from microscopic counts. Special Report No. 38, Department of
963 Oceanography, University of Washington.
964 Krom, M.D., Kress, N., Brenner, S., Gordon, L.I., 1991. Phosphorus limitation of primary
965 productivity in the eastern Mediterranean Sea. Limnology and Oceanography 36, 424-432.
966 Kühn, W., Pätsch, J., Thomas, H., Borges, A.V., Schiettecatte, L-S., Bozec, Y., Prowe, A.E.F.,
967 2010. Nitrogen and carbon cycling in the North Sea and exchange with the North Atlantic – A
968 model study, Part II: Carbon budget and fluxes. Continental Shelf Research 30, 1701-1716.
969 Leynaert, A., Tréguer, P., Lancelot, C., Rodier, M., 2001. Silicon limitation of biogenic silica
970 production in the Equatorial Pacific. Deep-Sea Research I 48, 639-660.
971 Lønborg, C., Davidson, K., Álvarez-Salgado, X.A., Miller, A.E.J., 2009. Bioavailability of bacterial
972 degradation rates of dissolved organic matter in a temperate coastal area during an annual cycle.
973 Marine Chemistry 113, 219-226.
974 Lomas, M.W., Burke, A.L., Lomas, D.A., Bell, D.W., Shen, C., Dyhrman, S.T., Ammerman, J.W.,
975 2010. Sargasso Sea phosphorus biogeochemistry: an important role for dissolved organic
976 phosphorus (DOP). Biogeosciences 7, 695-710.
977 Lopez, J., Garcia, N.S., Talmy, D., Martiny, A.C., 2016. Diel variability in the elemental
978 composition of the marine cyanobacterium *Synechococcus*. Journal of Plankton Research 38,
979 1052-1061.
980 López-Sandoval, D.C., Fernández, A., Marañón, E., 2011 Dissolved and particulate primary
981 production along a longitudinal gradient in the Mediterranean Sea. Biogoesciences 8, 815-825.

Mayers, K.M.J., Poulton, A.J., Daniels, C.J, Wells, S.R., Woodward, E.M.S., Tyrrell, T., Giering, S.L.C. Top-down control of coccolithophore populations during spring in a temperate Shelf Sea (Celtic Sea, April 2015). Progress in Oceanography, this issue.

Moore, C.M., Mills, M.M., Achterberg, E.P., Geider, R.J., LaRoche, J., Lucas, M.I., McDonagh, E.L., Pan, X., Poulton, A.J., Rijkenberg, M.J.A., Suggett, D.J., Ussher, S.J., Woodward, E.M.S., 2009. Large-scale distribution of Atlantic nitrogen fixation controlled by iron availability. Nature Geoscience 2, 867-871.

Moore, C.M., Mills, M.M., Arrigo, K.R., Berman-Frank, I., Bopp, L., Boyd, P.W., Galbraith, E.D., Geider, R.J., Guieu, C., Jaccard, S.L., Jickells, T.D., La Roche, J., Lenton, T.M., Mahowald, N.M., Maranon, E., Marinov, I., Moore, J.K., Nakatsuka, Oschlies, A., Saito, M.A., Thingstad, T.F., Tsuda, A., Ulloa, O., 2013. Nature Geoscience 6, 701-710, doi: 10.1038/ngeo1765.

Murphy, J., Riley, J.P., 1962. A modified single solution method for the determination of phosphate in natural waters. Analyticaa Chimica Acta 27, 31-36.

Pemberton, K., Rees, A.P., Miller, P.I., Raine, R., Joint, I., 2004. The influence of water body characteristics on phytoplankton diversity and production in the Celtic Sea. Continental Shelf Research 24, 2011-2028.

Popendorf, K.J., Duhamel, S., 2015. Variable phosphorus uptake rates and allocation across microbial groups in the oligotrophic Gulf of Mexico. Environmental Microbiology 17, 3992-4006.

Poulton, A.J., Sanders, R., Holligan, P.M., Stinchcombe, M.C., Adey, T.R., Brown, L., Chamberlain, K., 2006. Phytoplankton mineralization in the tropical and subtropical Atlantic Ocean. Global Biogeochemical Cycles 20, GB4002, doi: 10.1029/2006GB002712.

Poulton, A.J., Stinchcombe, M.C., Achterberg, E.P., Bakker, D.C.E., Dumousseaud, C., Lawson H.E., Lee, G.A., Richier, S., Suggett, D.J., Young, J.R., 2014. Coccolithophores on the north-west European shelf: calcification rates and environmental controls. Biogeosciences 11, 3919-3940.

Rees, A.P., Joint, I., Donald, K.M., 1999. Early spring bloom phytoplankton-nutrient dynamics at the Celtic Sea Shelf Edge. Deep-Sea Research I 46, 483-510.

Redfield, A.C., Ketchum, B.H., Richards, F.A., 1963. The influence of organisms on the composition of seawater. In: The sea (ed. Hill, M.N.), Wiley, 26-77.

Reynolds, S., Mahaffey, C., Roussenov, V., Williams, R.G., 2014. Evidence for production and lateral transport of dissolved organic phosphorus in the eastern subtropical North Atlantic. Global Biogeochemical Cycles 28, doi: 10.1002/2013GB004801.

Richier, S., Achterberg, E.P., Dumousseaud, C., Poulton, A.J., Suggett, D.J., Tyrrell, T., Zubkov, M.V., Moore, C.M., 2014. Phytoplankton responses and associated carbon cycling during

shipboard carbonate chemistry manipulation experiments conducted around Northwest European shelf seas. Biogeosciences 11, 4733-4752.

Scott, J.T., Cotner, J.B., LaPara, T.M., 2012. Variable stoichiometry and homeostatic regulation of bacterial biomass elemental composition. Frontiers in Microbiology 3, 1-8.

Siegal, D.A., Doney, S.C., Yoder, J.A., 2002. The North Atlantic spring phytoplankton bloom and Sverdrup's critical depth hypothesis. Science, 296, 730-733, doi: 10.1126/science.1069174.

Simpson J.H., Sharples, J., 2012. Introduction to the physical and biological oceanography of shelf seas. Cambridge, Cambridge University Press. 424 pp.

Sohm, J.A., Capone, D.G., 2010. Zonal differences in phosphorus pools, turnover and deficiency across the tropical North Atlantic Ocean. Global Biogeochemical Cycles 24, GB2008, doi: 10.1029/2008GB003414.

Stener, R.W., Elser, J.J., 2002. Ecological stoichiometry: The biology of elements from molecules to the biosphere. Princeton University, 464 pp.

Talmy, D., Blackford, J., Hardman-Mountford, N.J., Polimene, L., Follows, M.J., Geider, R.J., 2014. Flexible C:N ratio enhances metabolism of large phytoplankton when resource supply is intermittent. Biogeosciences 11, 4881-4895.

Tambi, H., Flaten, G.A.F., Egge, J.K., Bodtker, G., Jacobsen, T.F. Thingstad, 2009. Relationship between phosphate affinities and cell size and shape in various bacteria and phytoplankton. Aquatic Microbial Ecology Special Issue 3, 1-10.

Tarran, G.A., Heywood, J.L., Zubkov, M.V., 2006. Latitudinal changes in the standing stocks of nano- and pico-eukaryotic phytoplankton in the Atlantic Ocean. Deep-Sea Research II 53, 1516-1529.

Thingstad, T.F., Skjoldal E.F., Bohne, R.A., 1993. Phosphorus cycling and algal-bacterial competition in Sandsfjord, western Norway. Marine Ecology Progress Series 99, 239-259.

Thingstad, T.F., Riemann, B., Havskum, H., Garde, K., 1996. Incorporation rates and biomass content of C and P in phytoplankton and bacteria in the Bay of Aarhus (Denmark) June 1992. Journal of Plankton Research 18, 97-121.

Thingstad, T.F., Rassoulzadegan, F., 1999. Conceptual models for the biogeochemical role of the photic zone microbial food web, with particular reference to the Mediterranean Sea. Progress in Oceanography 44, 271-286.

Thomson-Bulldis, A., Karl, D.M., 1998. Application of a novel method for phosphorus determinations in the oligotrophic North Pacific Ocean. Limnology and Oceanography 43, 1565-1577.

Toggweiler, J.R., 1993. Carbon overconsumption. Nature 363, 210-211.

1051 Tomas, H., Bozec, Y., Elkalay, K., de Baaer, H.J.W., 2004. Enhanced open ocean storage of CO2
1052 from shelf sea pumping, Science 304, 1005-1008.
1053 Tomas, H., Bozec, Y., de Baar, H.J.W., Elkalay, K., Frankignoulle, M., Schiettecatte, L.-S.,
1054 Kattner, G., Borges, A.V., 2005. The carbon budget of the North Sea. Biogeosciences 2, 87-96.
1055 Venables, H.J., Moore, C.M., 2010. Phytoplankton and light limitation in the Southern Ocean:
1056 Learning from high-nutrient, high-chlorophyll areas. Journal of Geophysical Research, 115,
1057 C02015, doi: 10.1029/2009JC005361.
1058 Woodward, E.M.S., Rees, A.P., 2001. Nutrient distributions in an anticyclonic eddy in the North
1059 East Atlantic Ocean, with reference to nanomolar ammonium concentrations. Deep-Sea
1060 Research II, 48, 775-794.
1061 Widdicombe, C.E., Eloire, D., Harbour, D., Harris, R.P., Somerfield, P.J., 2010. Long-term
1062 phytoplankton community dynamics in the Western English Channel. Journal of Plankton
1063 Research 32, 643-655.
1064

1065 TABLES

1066 **Table 1.** Environmental characteristics at two study sites in the Celtic Sea for November (2014),
1067 April (2015) and July (2015). CCS, Central Celtic Sea study site; CS2, Shelf Edge study site;
1068 SML, surface mixed layer depth; SML Temp., average temperature of the SML; Zeup, depth of
1069 the euphotic zone; P_i, inorganic phosphate concentration; NO_x, concentration of nitrate+nitrite;
1070 N*, ratio of nitrate+nitrite to phosphate expressed after Moore et al. (2009); E_0, incidental
1071 irradiance (PAR) at the sea-surface; $\bar{E}_{SML}$, average irradiance (PAR) over the SML.

1072 **Table 2.** Euphotic zone inventories of biomass, production and phosphorus dynamics at two study
1073 sites in the Celtic Sea for November (2014), April (2015) and July (2015). CCS, Central Celtic
1074 Sea study site; CS2, Shelf Edge study site; Chl-*a*, chlorophyll-*a* concentrations; C_{phyto},
1075 phytoplankton biomass; C_{bact}, bacterial biomass; NPP, Net Primary Production; P_i, inorganic
1076 phosphate concentration; POP, particulate organic phosphate; DOP, dissolved organic
1077 phosphorus; P_i uptake, uptake of inorganic phosphate; DOP prod., production of DOP; PER,
1078 percentage extracellular release of DOP.

1079 **Table 3.** Turnover times and elemental stoichiometry at two study sites in the Celtic Sea for
1080 November (2014), April (2015) and July (2015). Stoichiometry of carbon fixation (net primary
1081 production, NPP) is expressed against P_i uptake and total P_i uptake (i.e. sum of P_i uptake + DOP
1082 production) on daily timescales. CCS, Central Celtic Sea study site; CS2, Shelf Edge study site;
1083 C_{phyto}, phytoplankton carbon; P_i, inorganic phosphate; POP, particulate organic phosphate; DOP,
1084 dissolved organic phosphorus; tP_i, total P_i uptake (sum of Pi-uptake and DOP production).

1085

1086 **SUPPLEMENTARY TABLES**

1087 **Table S1.** Irradiance in incubations.

Table 1. Environmental characteristics at two study sites in the Celtic Sea for November (2014), April (2015) and July (2015). CCS, Central Celtic Sea study site; CS2, Shelf Edge study site; SML, surface mixed layer depth; SML Temp., average temperature of the SML; Zeup, depth of the euphotic zone; P_i, inorganic phosphate concentration; NO_x, concentration of nitrate+nitrite; N*, ratio of nitrate+nitrite to phosphate expressed after Moore et al. (2009); E_0, incidental irradiance (PAR) at the sea-surface; $\bar{E}_{SML}$, average irradiance (PAR) over the SML.

Season / Date	Site	SML (m)	SML Temp. (^oC)	Zeup (m)	P_i (nmol P L^{-1})	NO_x (µmol N L^{-1})	N*	E_0	$\bar{E}_{SML}$ (mol PAR m^{-2} d^{-1})
					November 2014				
10 Nov	CCS	44	13.7	40	180	2.1	-0.8	8.4	1.6
12 Nov	CCS	32	13.6	28	180	2.1	-0.8	11.9	2.3
18 Nov	CS2	58	13.9	65	280	3.5	-1.0	7.7	1.8
20 Nov	CS2	58	14.1	55	220	2.6	-1.0	9.3	1.9
22 Nov	CCS	54	13.1	43	210	1.8	-1.6	8.1	1.4
25 Nov	CCS	52	12.8	50	210	2.5	-0.9	12.1	2.5
Mean		**50**	**13.5**	**47**	**213**	**2.4**	**-1.0**	**9.6**	**1.9**
					April 2015				
04 April	CCS	51	10.0	37	491	6.1	-1.8	20.7	3.3
06 April	CCS	47	10.0	37	459	5.7	-1.7	43.2	7.4
10 April	CS2	27	11.3	48	510	8.2	0.1	18.1	6.5
11 April	CCS	22	10.3	32	330	3.8	-1.5	42.3	12.8
15 April	CCS	25	10.6	28	190	1.2	-1.9	20.0	4.8
20 April	CCS	24	10.6	28	190	2.0	-1.0	41.4	10.3
24 April	CS2	24	11.7	30	190	2.3	-0.7	45.4	12.0
25 April	CCS	16	11.1	35	130	0.4	-1.7	42.0	17.5
Mean		**30**	**10.7**	**34**	**311**	**3.7**	**-1.7**	**34.1**	**9.3**
					July 2015				
14 July	CCS	28	16.0	53	90	<0.02	-1.4	23.2	8.7
15 July	CCS	30	16.1	52	90	<0.02	-1.4	33.2	11.6
19 July	CS2	11	15.8	20	70	<0.02	-1.1	26.1	9.5
20 July	CS2	12	16.2	25	80	0.17	-1.1	49.8	20.1
24 July	CCS	22	16.8	55	80	<0.02	-1.3	26.2	12.0
29 July	CCS	35	16.2	46	60	<0.02	-0.9	41.5	11.5
30 July	CCS	43	16.3	46	55	<0.02	-0.9	49.4	11.3
Mean		**26**	**16.2**	**42**	**76**	**0.04**	**-1.2**	**35.6**	**12.1**

Table 2. Euphotic zone inventories of biomass, production and phosphorus dynamics at two study sites in the Celtic Sea for November (2014), April (2015) and July (2015). CCS, Central Celtic Sea study site; CS2, Shelf Edge study site; Chl-*a*, chlorophyll-*a* concentrations; C_{phyto}, phytoplankton biomass; C_{bact}, bacterial biomass; NPP, Net Primary Production; P_i, inorganic phosphate concentration; POP, particulate organic phosphate; DOP, dissolved organic phosphorus; P_i uptake, uptake of inorganic phosphate; DOP prod., production of DOP; PER, percentage extracellular release of DOP.

Season / Date	Site	Chl-*a* (mg m^{-2})	C_{phyto} (mmol C m^{-2})	C_{bact} (mmol C m^{-2})	NPP (mmol C m^{-2} d^{-1})	P_i (mmol P m^{-2})	POP (mmol P m^{-2})	DOP (mmol P m^{-2})	P_i uptake (mmol P m^{-2} d^{-1})	DOP prod. (mmol P m^{-2} d^{-1})	PER (%)	Chl-*a* normalised NPP (gC (g Chl-*a*)$^{-1}$ h^{-1})
					November 2014							
10 Nov	CCS	59.7	91	28	37.0	7.6	1.7	14	0.24	-	-	0.8
12 Nov	CCS	37.4	36	-	18.5	5.2	-	-	0.14	0.19	58	0.7
18 Nov	CS2	54.4	78	24	22.5	18.3	2.0	25	0.30	0.28	48	0.6
20 Nov	CS2	57.6	73	24	26.3	12.0	1.4	13	0.24	0.11	31	0.6
22 Nov	CCS	68.7	91	32	42.9	9.0	1.0	11	0.25	0.13	34	0.8
25 Nov	CCS	70.8	93	32	46.9	10.5	1.1	19	0.25	0.17	34	0.9
Mean		**58.1**	**77**	**28**	**32.4**	**10.4**	**1.4**	**16**	**0.24**	**0.17**	**41**	**0.7**
					April 2015							
04 April	CCS	49.6	153	49	117.6	18.3	1.0	12	1.43	0.11	7	2.0
06 April	CCS	61.4	162	57	59.1	17.3	-	-	1.03	0.12	10	0.8
10 April	CS2	37.8	106	27	87.8	25.1	1.1	13	1.64	0.26	14	2.0
11 April	CCS	94.9	221	142	154.0	11.1	3.1	13	1.68	0.36	18	1.4
15 April	CCS	152.6	180	162	532.1	6.7	3.1	10	2.08	0.65	24	3.0
20 April	CCS	92.3	168	182	206.2	5.3	2.4	9	1.89	0.82	30	1.9
24 April	CS2	57.4	202	44	132.8	5.7	2.1	6	1.33	1.11	45	2.0
25 April	CCS	110.4	247	142	321.0	5.7	3.5	12	1.76	0.48	21	2.5
Mean		**82.1**	**180**	**101**	**201.3**	**11.9**	**2.3**	**11**	**1.61**	**0.49**	**21**	**2.0**
					July 2015							
14 July	CCS	19.3	200	30	58.5	6.3	2.2	7	1.11	0.02	2	2.3
15 July	CCS	28.5	121	23	43.7	6.6	-	-	1.18	-	-	1.2
19 July	CS2	18.4	66	32	32.5	1.8	1.0	3	0.72	0.04	5	1.3
20 July	CS2	17.2	-	-	18.3	2.1	-	-	0.53	0.03	5	0.8
24 July	CCS	35.7	86	33	38.3	12.2	-	-	0.96	0.07	7	0.8
29 July	CCS	26.4	79	27	19.7	4.2	1.3	10	0.92	0.08	8	0.6
30 July	CCS	28.0	-	-	36.8	5.3	-	-	0.48	0.06	11	1.0
Mean		**24.8**	**110**	**29**	**35.4**	**5.5**	**1.5**	**7**	**0.84**	**0.05**	**6**	**1.1**

Table 3. Turnover times and uptake stoichiometry at two study sites in the Celtic Sea for November (2014), April (2015) and July (2015). Stoichiometry of carbon fixation (net primary production, NPP) is expressed against P_i uptake and total P_i uptake (i.e. sum of P_i uptake + DOP production) on daily timescales. CCS, Central Celtic Sea study site; CS2, Shelf Edge study site; C_{phyto}, phytoplankton carbon; P_i, inorganic phosphate; POP, particulate organic phosphate; DOP, dissolved organic phosphorus; tP_i, total P_i uptake (sum of P_i-uptake and DOP production).

Season / Date	Site	C_{phyto}	P_i	POP	DOP	Daily NPP:P_i uptake	Daily NPP:tPi uptake
		[d^{-1}]				[mol C:mol P]	
				November 2014			
10 Nov	CCS	1.5	21.9	4.9	-	154	-
12 Nov	CCS	1.9	25.7	-	-	132	56
18 Nov	CS2	2.2	42.3	4.6	62	75	37
20 Nov	CS2	2.0	34.7	4.0	83	110	75
22 Nov	CCS	1.5	25.0	2.8	59	172	113
25 Nov	CCS	1.4	29.1	3.0	102	188	123
Mean		**1.7**	**29.8**	**3.9**	**77**	**132**	**81**
				April 2015			
04 April	CCS	0.7	8.9	0.5	78	82	76
06 April	CCS	1.7	11.6	-	-	57	51
10 April	CS2	0.7	10.6	0.5	35	54	46
11 April	CCS	1.0	4.6	1.3	24	92	75
15 April	CCS	0.5	2.2	1.0	11	256	195
20 April	CCS	0.7	1.9	0.9	8	109	76
24 April	CS2	0.7	3.0	1.1	4	100	54
25 April	CCS	0.6	2.2	1.4	17	182	143
Mean		**0.8**	**5.6**	**0.9**	**25**	**116**	**90**
				July 2015			
14 July	CCS	1.1	3.9	1.4	239	53	52
15 July	CCS	2.1	3.9	-	-	37	-
19 July	CS2	1.9	1.7	1.0	45	45	43
20 July	CS2	3.1	2.7	-	-	35	33
24 July	CCS	3.1	8.8	-	-	40	37
29 July	CCS	4.4	3.2	1.0	88	21	20
30 July	CCS	2.5	7.7	-	-	77	68
Mean		**2.6**	**4.6**	**1.1**	**124**	**44**	**42**

Poulton et al., P-dynamics, PiO Supplementary Table S1

Percentage Light Depth	LED Panels	Neutral density type (% transmission)	Measured Irradiance (µmol quanta m^{-2} s^{-1})	Target Photon flux (mol quanta m^{-2} d^{-1})	Actual Photon flux (mol quanta m^{-2} d^{-1})	(mol quanta m^{-2} h^{-1})
November 2015 (photoperiod = 9 h; E_0 = 8.7 mol quanta m^{-2} d^{-1})						
60%	2	2 x 0.15 ND (69%)	167	5.2	5.4	0.60
40%	1	None	147	3.5	4.8	0.53
20%	1	0.30 ND (51%)	70	1.7	2.3	0.25
10%	1	0.15 ND (69%)	26	0.9	0.8	0.09
5%	1	0.9 ND (14%)	15	0.4	0.5	0.05
s1%	1	1.2 ND (7%)	7	0.1	0.2	0.03
April 2015 (photoperiod = 14 h; E_0 = 33.9 mol quanta m^{-2} d^{-1})						
60%	3	None	440	20.3	22.2	1.58
40%	3	1 x 0.15 ND (69%)	260	13.5	13.1	0.94
20%	3	3 x 0.3 ND (51%)	120	6.8	6.0	0.43
10%	1	0.3 ND (51%)	68	3.4	3.4	0.24
5%	2	2 x 0.9 ND (14%)	21	1.7	1.1	0.08
1%	1	1.2 ND (7%)	7	0.3	0.4	0.03
July 2015 (photoperiod = 16 h; E_0 = 39.8 mol quanta m^{-2} d^{-1})						
60%	3	None	440	23.9	25.3	1.58
40%	3	1 x 0.15 ND (69%)	260	15.9	15.0	0.94
20%	3	3 x 0.3 ND (51%)	120	8.0	6.9	0.43
10%	1	0.3 ND (51%)	68	4.0	3.9	0.24
5%	2	2 x 0.9 ND (14%)	21	2.0	1.2	0.08
1%	1	1.2 ND (7%)	7	0.4	0.4	0.03

FIGURES

Figure 1. Location of the sampling stations in the Celtic Sea for this study: CCS, Central Celtic Sea site; CS2, Shelf edge site.

Figure. 2. Box and whisker plots of: (a) phosphate (P_i) concentration (nmol P L^{-1}); (b) chlorophyll-*a* (Chl-*a*) concentration (mg m^{-3}); (c) dissolved organic phosphorus (DOP) concentration (nmol P L^{-1}); and (d) particulate organic phosphorus (POP) concentration (nmol P L^{-1}). Plots show median (solid line), as well as the 10^{th}, 25^{th}, 75^{th} and 90^{th} percentiles.

Figure 3. Box and whisker plots of: (a) phosphate (P_i) uptake (nmol P L^{-1} h^{-1}); and (b) the ratio of light to dark P_i-uptake (L:D). Dashed line on (b) indicates 1:1. Plots show median (solid line), as well as the 10^{th}, 25^{th}, 75^{th} and 90^{th} percentiles.

Figure. 4. Box and whisker plots of: (a) dissolved organic phosphorus (DOP) production (nmol P L^{-1} h^{-1}); (b) the ratio of light to dark P_i-uptake (L:D); and (c) dissolved organic phosphorus (DOP) production expressed as a percentage of total P_i-uptake (Percentage Extracellular Release, PER). Dashed line on (b) indicates 1:1. Plots show median (solid line), as well as the 10^{th}, 25^{th}, 75^{th} and 90^{th} percentiles.

Figure 5. Time-series measurements of P_i uptake for two temporal experiments: (a) hourly P_i-uptake rates at 4 h time points over 24 h; and (b) cumulative P_i-uptake over 24 h. Dashed vertical lines indicate sunset (21:00 GMT) and sunrise (05:00 GMT). Cumulative P_i-uptake was 17.1 nmol P L^{-1} d^{-1} and 22.7 nmol P L^{-1} d^{-1}, respectively.

SUPPLEMENTARY FIGURES

S1. Size-fractionated Pi-uptake for surface waters at three sites in the Celtic Sea.